AD A084 ...

AFGL-TR-79-0253
ENVIRONMENTAL RESEARCH PAPERS, NO. 679

Atmospheric Attenuation of Millimeter and Submillimeter Waves: Models and Computer Code

VINCENT J. FALCONE, JR.
LEONARD W. ABREU
ERIC P. SHETTLE

15 October 1979

OPTICAL PHYSICS DIVISION PROJECT 7670
AIR FORCE GEOPHYSICS LABORATORY
HANSCOM AFB, MASSACHUSETTS 01731

AIR FORCE SYSTEMS COMMAND, USAF

This report has been reviewed by the ESD Information Office (OI) and is releasable to the National Technical Information Service (NTIS).

This technical report has been reviewed and is approved for publication.

FOR THE COMMANDER

John Howard

Chief Scientist

Qualified requestors may obtain additional copies from the Defense Documentation Center. All others should apply to the National Technical Information Service.

Unclassified

SECURITY CLASSIFICATION OF THIS PAGE (When Data Entered)

REPORT DOCUMENTATION PAGE		READ INSTRUCTIONS BEFORE COMPLETING FORM
1. REPORT NUMBER AFGL-TR-79-0253	2. GOVT ACCESSION NO. AD A084455	3. RECIPIENT'S CATALOG NUMBER
4. TITLE (and Subtitle) ATMOSPHERIC ATTENUATION OF MILLIMETER AND SUBMILLIMETER WAVES: MODELS AND COMPUTER CODE		5. TYPE OF REPORT & PERIOD COVERED Scientific. Interim.
		6. PERFORMING ORG. REPORT NUMBER ERP No. 679
7. AUTHOR(s) Vincent J. Falcone, Jr. Leonard W. Abreu Eric P. Shettle		8. CONTRACT OR GRANT NUMBER(s)
9. PERFORMING ORGANIZATION NAME AND ADDRESS Air Force Geophysics Laboratory (OPI) Hanscom AFB Massachusetts 01731		10. PROGRAM ELEMENT, PROJECT, TASK AREA & WORK UNIT NUMBERS 62101F 76701301
11. CONTROLLING OFFICE NAME AND ADDRESS Air Force Geophysics Laboratory (OPI) Hanscom AFB Massachusetts 01731		12. REPORT DATE 15 October 1979
		13. NUMBER OF PAGES 76
14. MONITORING AGENCY NAME & ADDRESS (if different from Controlling Office)		15. SECURITY CLASS. (of this report) Unclassified
		15a. DECLASSIFICATION/DOWNGRADING SCHEDULE

16. DISTRIBUTION STATEMENT (of this Report)

Approved for public release; distribution unlimited.

17. DISTRIBUTION STATEMENT (of the abstract entered in Block 20, if different from Report)

18. SUPPLEMENTARY NOTES

19. KEY WORDS (Continue on reverse side if necessary and identify by block number)

Attenuation, Millimeter waves, Submillimeter waves, Microwave, Precipitation, Rain models, Cloud models, Fog models, Mie scattering and Computer codes

20. ABSTRACT (Continue on reverse side if necessary and identify by block number)

Atmospheric attenuation of millimeter and submillimeter waves is calculated for clear, fog, cloud and rain atmospheres. The frequency range considered is 1-1000 GHz. The clear atmospheres transmission spectra is calculated by a computer efficient algorithm of AFGL's HITRAN code. This new code is called FASCODE-1. The hydrometeor attenuation of fog, clouds and rain (precipitation), calculated by Mie scattering is addended to FASCODE-1. Models of fog, clouds and rain typical of mid-latitude temperate regions are used in calculations of transmission and attenuation.

DD FORM 1 JAN 73 1473 EDITION OF 1 NOV 65 IS OBSOLETE

Unclassified

SECURITY CLASSIFICATION OF THIS PAGE (When Data Entered)

409578

Preface

The authors would like to acknowledge the useful suggestions received from Donald Grantham, Iver Lund, and Arthur Kantor of AFGL/LY and to Dr. E.T. Florance, ONR, Pasadena, CA for his interpolation algorithm AITK.

We also thank Dr. P. Ray, National Severe Storm Laboratory, Norman, Oklahoma for his program INDEX.

Contents

Illustrations

Tables

Atmospheric Attenuation of Millimeter and Submillimeter Waves: Models and Computer Code

1. INTRODUCTION

The increasing use of microwaves in the past few years by DOD for determination of geophysical parameters, high data rate communication channels, weapons guidance and target acquisition has emphasized the need for better modelling and more accurate calculations of attenuation through clear and hydrometeor laden atmospheres. To fulfill this need, the use of millimeter and submillimeter wavelengths show many advantages over the use of microwaves:

a. better sensitivity to geophysical parameters
b. larger communication bandwidths
c. more secure communications
d. narrower beamwidths
e. good angular resolution
f. imagery capability

One disadvantage is atmospheric attenuation caused by gaseous absorption and extinction by hydrometeors.

The objective of this report is to model and calculate atmospheric transmissions and atmospheric attenuation of radio frequency waves in the spectral region of 1-1000 GHz, that is, 30-.03 cm wavelengths or .30-33 cm^{-1} (wave numbers).

(Received for publication 15 October 1979)

This report follows in the spirit of the original atmospheric transmission models by McClatchey et al,[1] which were developed into the LOWTRAN transmission code,[2] an operationally directed computer code for user implementation.*

The models used in this study are the Clear Atmosphere Model given in Valley,[3] the Fog and Cloud Models from Silverman[4] and the research of the authors (texts by Mason[5] and Borovikov[6] were extensively utilized), and the Rain Models which were generated from the research of the authors. The rainfall rates considered are from 0.25 mm/hr to 150 mm/hr. The dropsize distribution of these rainfall rates is determined from the Marshall-Palmer distribution.

The use of these models should not be interpreted as if these are the only models of use in propagation studies. The models were chosen because they are representative of midlatitude conditions. The computer program given in Appendix D will allow each researcher to calculate transmittance and/or attenuation for any horizontally stratified model which represents real world conditions.

Table 1 lists the definitions for the spectral region c the electromagnetic spectrum that will be employed in this report.

Table 1. Spectra Designations

Region	Wavelength	Frequency
Microwave	1 m-1 cm	.30GHz-30GHz
Millimeter	1 cm-0.1 cm	30-300
Submillimeter	0.1 cm-0.01 cm	300-3000

*The codes described in this report are available from National Climatic Center, Federal Building, Asheville, NC 28801 for a service charge.

1. McClatchey, R.A., Fenn, R.W., Selby, J., Volz, F.E., and Garing, J.S. (1972) Optical Properties of the Atmosphere (3rd Ed.), AFCRL-72-0497, AD

2. Selby, J.E.A. and McClatchey, R.A. (1972) Atmospheric Transmission From 0.25 to 28.3 um: Computer Code LOWTRAN 2, AFCRL-72-0745, AD

3. Valley, S.L. (Editor) (1965) Handbook of Geophysics and Space Environments, AFCRL.

4. Silverman, B.A. and Sprague, E.D. (1970) Airborne Measurements of In-Cloud Visibility, National Conference on Weather Modification of the American Meteorological Society, April 6-9, Santa Barbara, California.

5. Mason, B.J. (1971) The Physics of Clouds, Clarendon Press, Oxford.

6. Borovikov, A.M., Khrgian, A.K.H. and others (1963) Cloud physics, U.S. Department of Commerce, Office of Technical Services.

The term radio frequency encompasses the microwave, millimeter and submillimeter frequency bands.

In the 1-1000 GHz frequency range considered, the clear atmosphere attenuation is due primarily to the rotational absorption lines of water vapor (H_2O) and oxygen (O_2). If one were mainly interested in communication channels, only water vapor and oxygen are needed to account for clear air attenuation. However, the application of this research in addition to communication is the identification of geophysical parameters, ground target acquisition and weapons guidance. These applications require the additional absorption lines of ozone (O_3) carbon monoxide (CO) and nitrous oxide (N_2O) for completeness and accuracy.

Since the AFGL HITRAN data base and computational technique of McClatchey et al[7] was originally generated by specialists in the infrared region, there exist differences in notation between it and the notation employed by the microwave specialists. In the infrared region, the specialists use transmittance to describe propagation, whereas in the microwave region the specialists use attenuation to describe propagation (see Appendix A for definitions).

One major point of this research is that systems designers have to adjust their ideas of completely deterministic propagation models and rethink system propagation as being statistical in nature. In the microwave region the atmosphere is essentially static (that is, at most, rain conditions have to be considered for frequencies above 10 GHz). As systems go higher in frequency through the millimeter and submillimeter bands, the clear atmosphere attenuates due to water vapor, oxygen, ozone and other minor constituent gases. In addition to the clear atmosphere, fog, clouds and rain attenuate by both scattering (deflection of energy) and absorption (dielectric heating of water drops). It is the statistics of the meteorological conditions of gaseous atmospheric concentrations, and hydrometeor fog, clouds and rain that have to be considered when designing millimeter and submillimeter systems.

2. CLEAR ATMOSPHERE

The atmospheric molecular absorption spectra is calculated by a computer efficient algorithm of AFGL's HITRAN Code. This new code was advanced by Clough et al.[8] It is called FASCOD-1, an acronym for Fast Atmospheric

---

7. McClatchey, R.A., Benedict, W.S., Clough, S.A., Burch, D.E., Calfee, R.F., Fox, K., Rothman, L.S. and Garing, J.S. (1973) AFCRL Atmospheric Absorption Line Parameters Compilation, AFCRL-TR-73-0096, AD

8. Clough, S.A. et al. (1980) FASCOD-1, AFGL Technical Report, to be published.

Signature Code. The HITRAN code is a compilation of spectral line parameters of the significant atmospheric absorption lines for frequencies from the microwave through the infrared regions of the spectrum. As previously stated, the molecules of interest in the 1-1000 GHz region are oxygen (O_2), water vapor (H_2O), ozone (O_3), carbon monoxide (CO), and nitrous oxide (N_2O). The paper by Clough et al[8] should be consulted for further information about this program and the theory of clear air transmission.

3. HYDROMETEORS

Haze, fog, and clouds are intimately related. As is well-known the atmosphere is never free of particles (aerosols). Haze is an aerosol; it is composed of hygroscopic and non-hygroscopic particles. The hygroscopic particles act as nuclei for condensation of water vapor. In essence, fog, clouds and thus, precipitation are the meteorological results of nuclei that began as haze. The transmittance and attenuation due to hydrometeors (fog, clouds and rain) is calculated by the full Mie theory. The only distinction between fog and clouds is their distance from the earth. Similarly, the distinction between clouds (or fog) and rain is almost non-existent when they are mixed. For conciseness, the terms fog, cloud and rain have to be defined. In this report, the radar meteorologists' definition will be adhered to. Fog and clouds refer to a collection of water drops with diameter less than 100 μm, [N.B. this report uses radius instead of diameter; thus the collection of water drops with radii less than 50 μm or 0.05 mm]. Rain refers to a collection of water drops with diameters up to 6.5 mm (or radii up to 3.3 mm).

It is assumed that the hydrometeors are homogeneous, spherical masses of pure water, with a density slightly less than 1 g/cm^3. A quick observation of these definitions is that the fog and cloud droplets are much smaller than the wavelengths considered in this report. It will be shown later that in this case, the Rayleigh approximation holds ($x = 2\pi r/\lambda \ll 1$), and the attenuation of the fog or cloud is directly proportional to the liquid water content (see Eq. (21)). On the other hand, rain attenuation requires the full Mie theory calculations. It is assumed that the raindrop spectra has the distribution first advanced by Marshall and Palmer[9] (M-P). The choice of M-P distribution is made for the following reasons:

a. The rain parameter measured by meteorologists is the rainfall rate R, but the parameter of importance in scattering calculations is dropsize distribution.

9. Marshall, J.S. and Palmer, W.M.K. (1948) The distribution of raindrops with size, J. Meteor. 5:165-166.

The M-P distribution n(r) is explicitly related to rainfall rate R (see Eqs. (22) and (23)).

b. The M-P distribution has a negative exponential form, which is the general form of other "accepted" distributions. Specifically, the same form as the Deirmendjian[10] modified gamma function distribution used in modelling cloud and rain droplet distributions where $\gamma = 1$ (see Eq. (15)).

c. The amplitude factor in the M-P distribution is a constant for rainfall for continuous rain conditions (see Table 6).

d. Many researchers are currently employing the M-P distribution, so it is already accepted by the research community.

4. CALCULATIONS

4.1 Clear Atmosphere Transmission/Attenuation

In the frequency range 1-1000 GHz the clear atmosphere progresses from 100 percent transparent to opaque as the frequency is increased. This transmission and attenuation is present 100 percent of the time (see Figures 1, 2, 3 and 4). Clough et al[8] discusses the clear air transmittance.

4.2 Hydrometeors' Attenuation

The transmittance/attenuation of millimeter and submillimeter waves by hydrometeors is appreciable for a significant percentage of a year. Consequently, estimates of fog, cloud and rain attenuation are required for the design of various systems. Physically, extinction (IR notation which is equivalent to attenuation in microwave notation), the removal of energy from an electromagnetic wave, is the sum of two processes. The first is absorption (Q_a) which arises from the dielectric heating of condensed water by the incident electromagnetic wave, and the second is scattering (Q_s) which arises from scattering of the incident electromagnetic wave into other directions (see Eq. (1)). It should be noted that the scattering term includes radiation that is scattered into the foreward direction as well as into other directions. The attenuation due to frozen (ice) hydrometeors is not considered in this report, since the imaginary component of the index of refraction is small and thus the attenuation is small. Stated differently, natural ice clouds, hail and snow are highly transparent to passive radiowave measurements. It is safe to say that the theory of calculation of scattering by hydrometeors is well known (see Figure 5). However, the meteorological statistics of hydrometeors are not well known. This latter fact leads to difficulties in modelling as will be shown below.

10. Deirmendjian, D. (1969) Electromagnetic Scattering on Polydispersions, Elsevier Publishing Co.

The theory of Mie scattering is given in many excellent texts, Deirmendjian,[10] Van de Hulst[11] and Kerker.[12] The theory employed in this report is primarily based on the work of Deirmendjian; a short review follows.

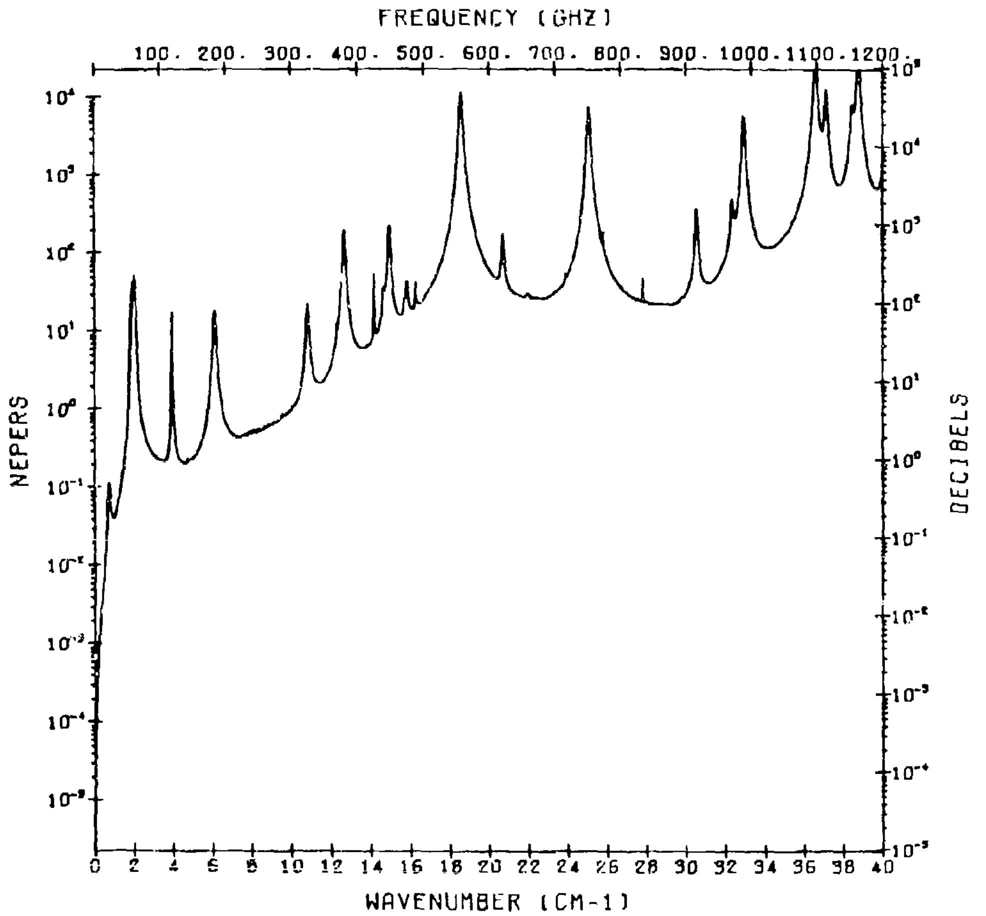

Figure 1. Zenith Attenuation (Nepers, Decibels) Through the Entire Atmosphere (U.S. Standard) as a Function of Frequency (cm^{-1}, GHz). Attenuation for angles other than zenith may be calculated by multiplying the attenuation (Figure 1) times the secant of the zenith angle.

---

11. Van DeHulst, H.C. (1957) Light Scattering by Small Particles, John Wiley & Sons Inc.

12. Kerker, M. (1969) The Scattering of Light and Other Electro-Magnetic Radiation, Academic Press.

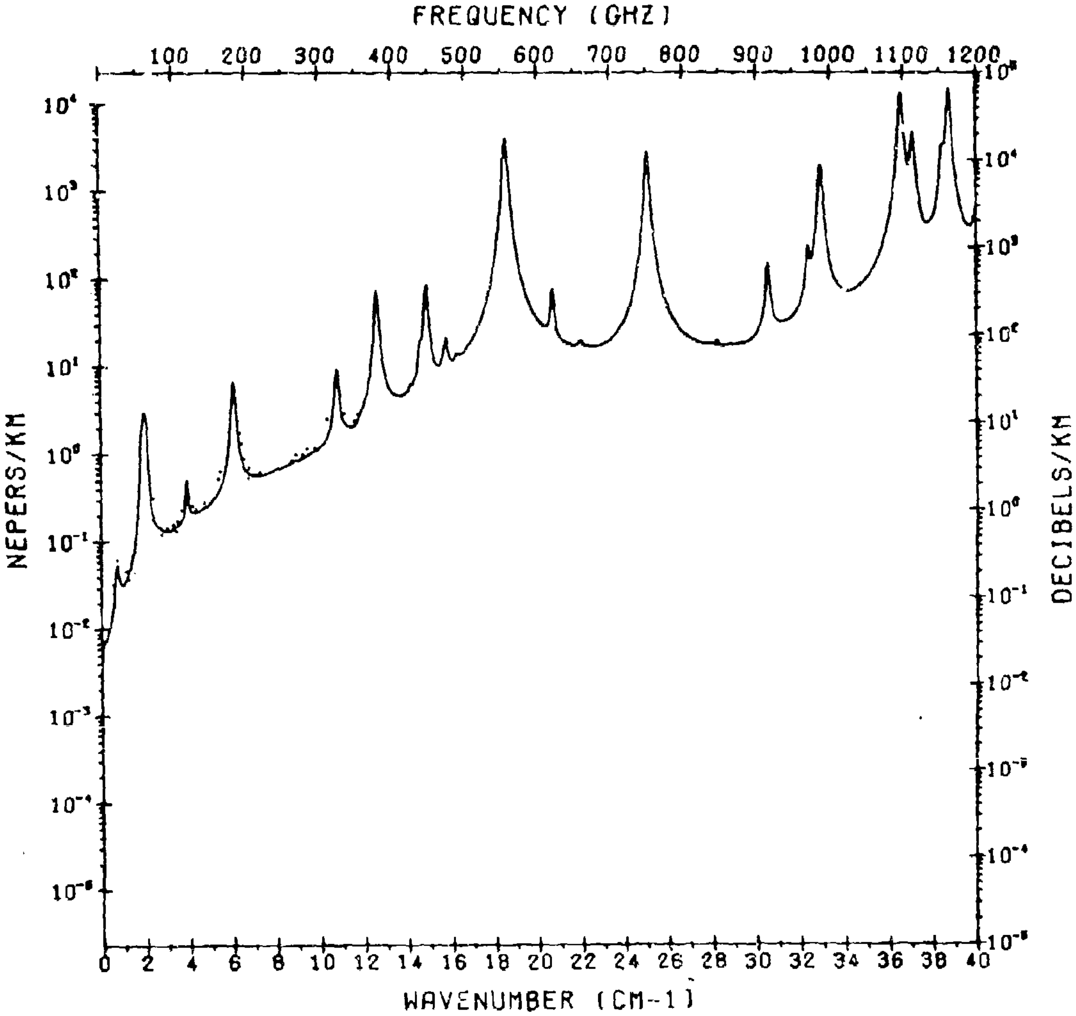

Figure 2. The Attenuation Through a 1 km Thick Clear Atmosphere at 20°C Temperature and 1013 mb Pressure. Horizontal or near horizontal path attenuation may be calculated using this figure. Experimental measurements are represented by dots

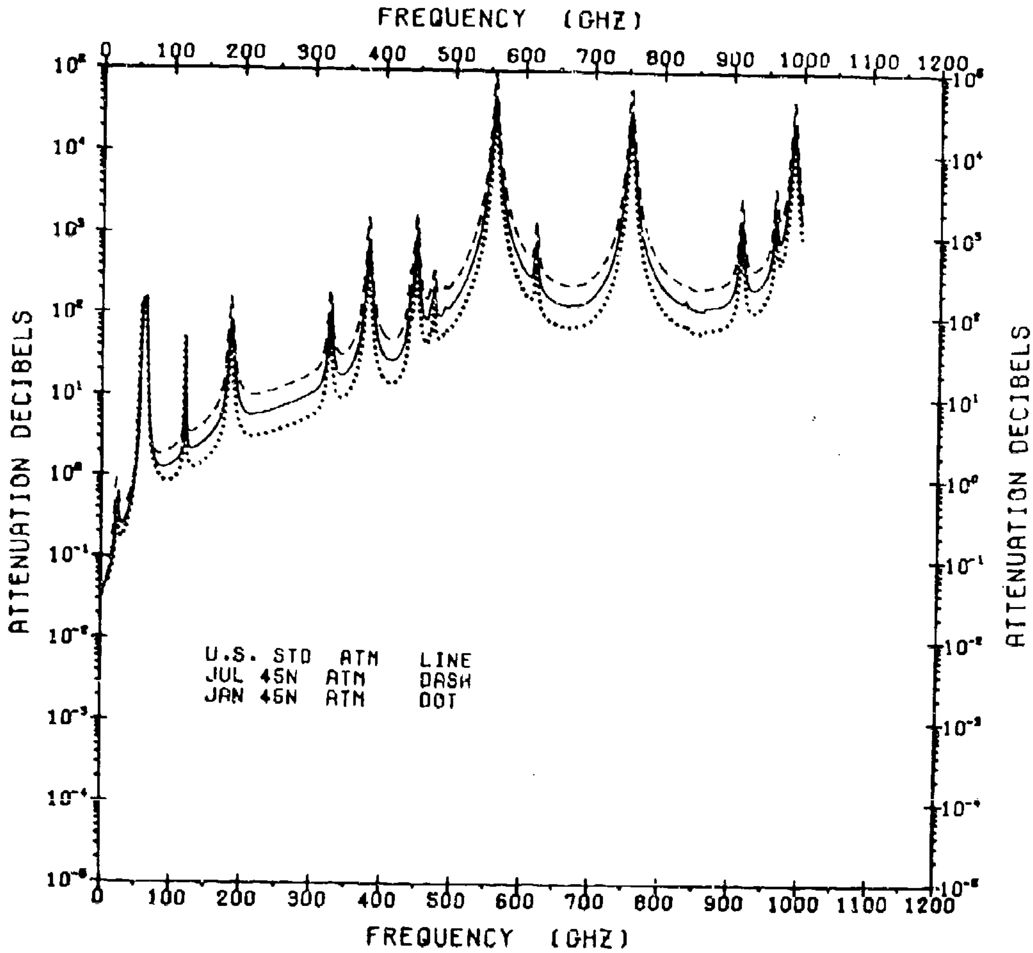

Figure 3. Zenith Attenuation Through Different Atmospheres as a Function of Frequency. The U.S. Standard Atmosphere and the midlatitude (45°N) model atmospheres for July and January are from Valley.[3] This figure delineates attenuation due to seasonal atmospheric changes

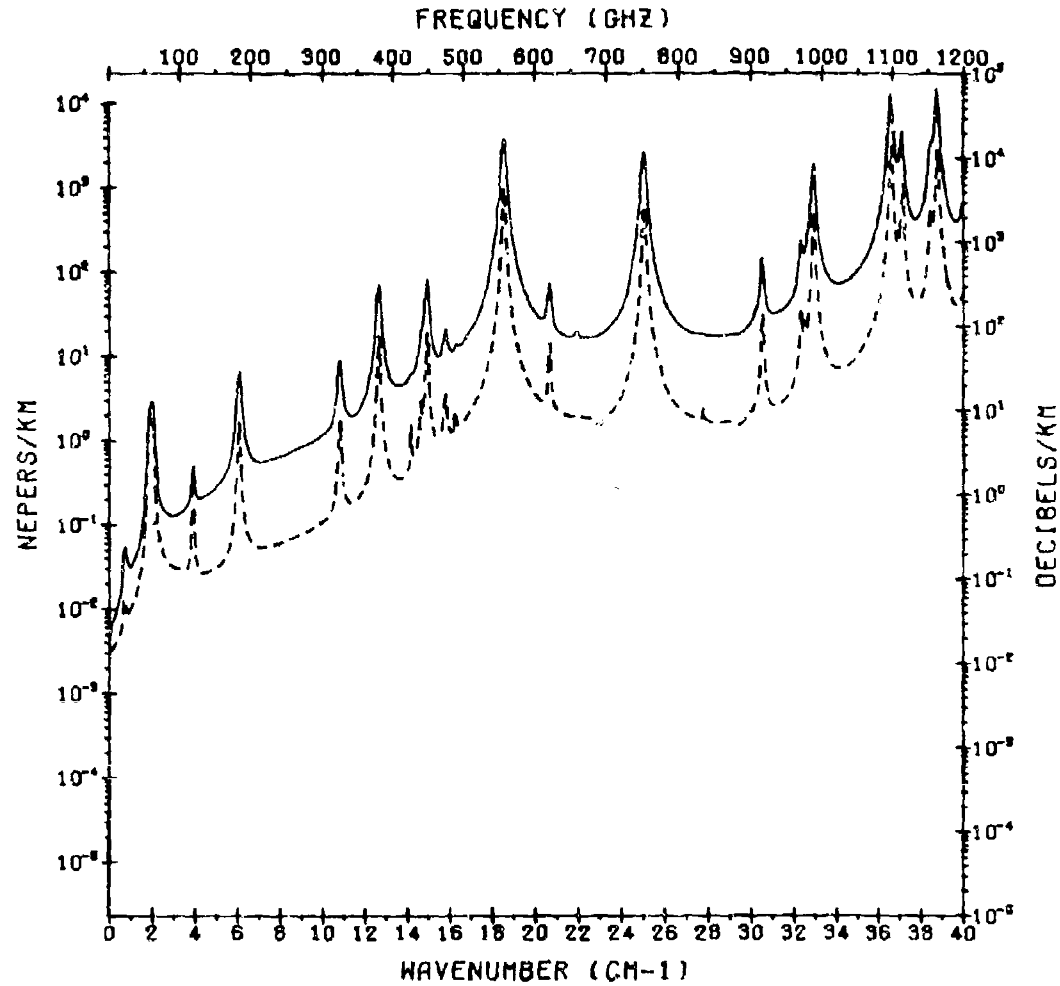

Figure 4. The Attenuation Through a 1 km Thick Atmosphere at Sea Level (20°C, 1013 mb) and 4 km (0°C, 628 mb). This figure relates attenuation decrease with altitude

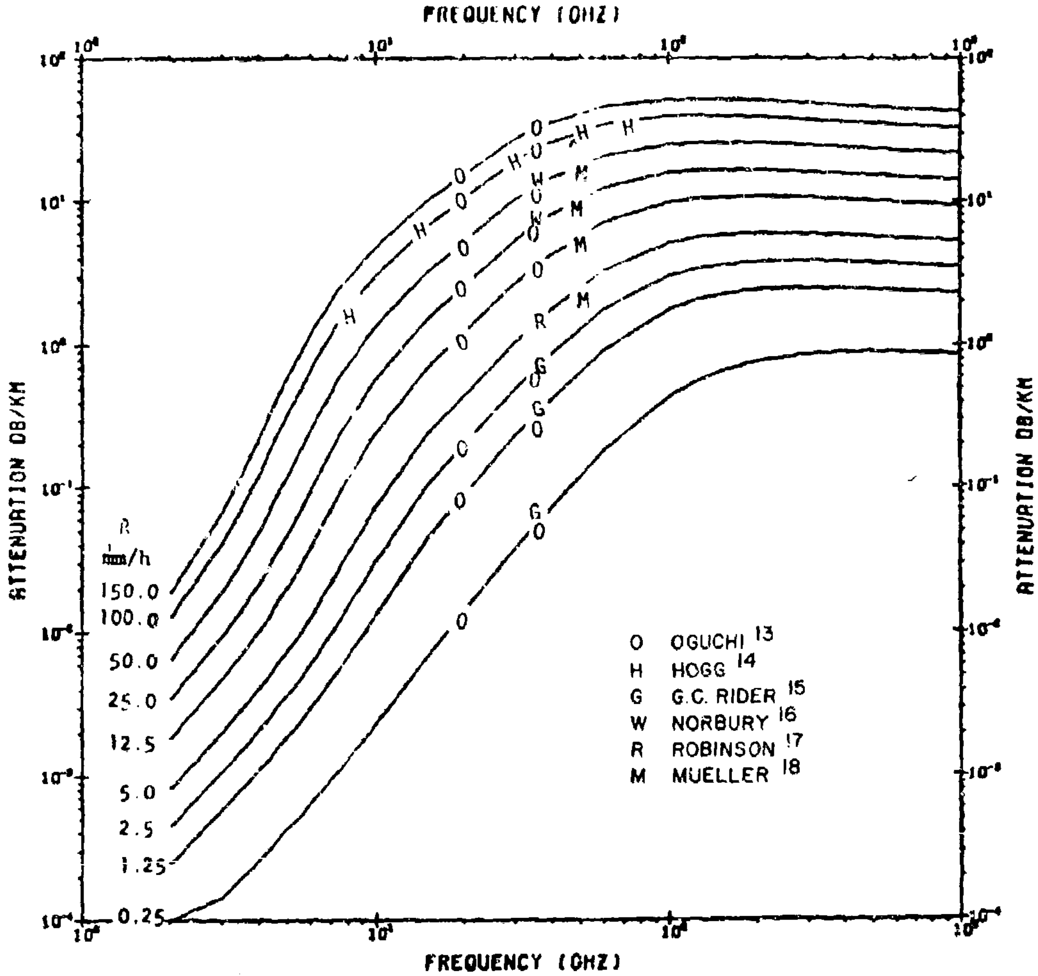

Figure 5. Attenuation vs Frequency for Rainfall Rates, 0.25, 1.25, 2.50, 5.00, 12.50, 25.50, 100 and 150 mm/hr for 20°C temperature drops employ the Marshall-Palmer distribution. Experimental data verifying theoretical calculations are noted. The experiments measured both attenuation (dB/km) and the rainrate (mm/hr). Oguchi's calculations are included for comparison

---

Due to the number of references to be included as footnotes on this page, the reader is referred to the list of references, page 53.

In most scattering calculations it is assumed, as in this report, that the shape of hydrometeors is approximately spherical and their temperature is homogeneous. These two assumptions are true for fog and clouds. When water particles (fog and clouds) are small, that is, .01-10 μm in radius the ratio of their surface to mass is large, of the order of 10^6-10^3 respectively. This means that small water particles respond rapidly to changes in temperature. Rain behaves differently; it is a well known fact that raindrop shape depends on the drop radius and the conditions of fall. Raindrops smaller than 1 mm in radius tend to be spherical. Drops approximately 1.5 mm and larger, falling in stagnant air, tend to be flat or even concave at the base and slightly rounded at the top, whereas drops ($\sim$ 1.5 mm), falling in turbulent air, tend to be ellipsoidal.[5] Jones[19] studied the shape of raindrops in naturally occurring rain and has classified them as spherical, oblate and prolate spheroids, and irregular ellipsoids. The large drops, he concluded, oscillated about a preferred shape. Oguchi[20] calculated scattering from spheroids. A general theory for other shapes does not exist. Rain has a surface-to-mass ratio of the order of 10 (which means it does not respond rapidly to changes in temperature) so that, as the drop falls, heat transfer between the drop and its environment is taking place. Thus, the temperature of a raindrop is not homogeneous because of this heat transfer between the drop and its environment.

Other implicit rain assumptions are that the drops are not electrically charged, and that the drops do not cluster together. This latter assumption ignores the fact that raindrops are not uniformly dispersed in the atmosphere, even though there is evidence to show that raindrops tend to group. The usual assumption made is that the drops are far enough apart to have negligible interaction between them.[21] The dual assumption of spherical drops and homogeneous temperatures of drops has been made to simplify calculations.

The drops of liquid water in fog, clouds and rain absorb, scatter and emit thermal radiation at radiowave frequencies. The absorption and scattering properties of a single dielectric sphere was first advanced by Mie.[22] Fog, clouds and rain are not composed of a single size drop, but are a composition of a distribution of many sizes. If this distribution of dropsize radii is known, then the Mie theory

---

19. Jones, D.M.A. (1959) The shape of raindrops, J. Meteor. 16:504-510.

20. Oguchi, T. (1960) (1964) Attenuation of electromagnetic wave due to rain with distorted raindrops, J. Radio Res. Lab. (Japan) 7:467, Part II, J. Radio Res. Lab. 11:19.

21. Lu'e, G.D. (1968) Penetrability of haze, fog, clouds and precipitation by radiant energy over the spectral range 0.1 micron to 10 centimeters, NAVWAG Study 61, AD 847658, Maj.

22. Mie, G. (1908) Beitrage zur optik truber medien, speziell kollodaler metallosungen, Ann der Phys. 25:377-445.

may be used to calculate the exact absorption and scattering properties. An excellent review and application paper was published by Gunn and East,[23] applying the Mie Theory to the scattering of microwaves by liquid and solid hydrometeors. A limitation of the Gunn and East work is that they considered only those frequencies of use to radar.

In the Mie Theory, the following terms are defined for the scattering of a plane wave by a homogeneous, dielectric sphere (pure water sphere in this research). The extinction cross-section Q_{ext} (L^2) is the sum of the absorption cross-section Q_a and the scattering cross-section Q_s, (where L is the unit of length)

$$Q_{ext} = Q_a + Q_s \tag{1}$$

The extinction cross-section is defined such that Q_{ext} multiplied by the incident power yields the total power extracted by an obstacle, either by absorption, scattering, or both, from the incident plane wave.

Suppose that W_i is the incident power density (Watts L^{-2}) upon the droplet. The extinction cross-section is the ratio of the total power P(watts) extracted to the incident power density

$$Q_{ext} = \frac{P}{W_i} (L^2) \tag{2}$$

In the Mie Theory the scattering coefficients are expressed in terms of a dimensionless size parameter $x = kr$, where $k = 2\pi/\lambda$ is the free space propagation constant and r is the radius of the sphere

$$x = \frac{2\pi r}{\lambda}$$

λ is the wavelength of incident radiation surrounding the particle. The physical importance of the particle radius and the wavelength is that these two parameters determine the distribution of phase over a particle. This is seen from the incident electric field $E_{inc} = \exp[-i(kr - \omega t)]$. When the radius of the particle is much less than a wavelength, the phase of the incident wave is uniform over the particle (Rayleigh scatter). When the size of the particle is comparable to a wavelength, the phase of the incident wave is not uniform over the particle, and there results spacial and temporal phase differences. These differences exhibit themselves as

---

23. Gunn, K. L. S. and East, T. W. R. (1954) The microwave properties of precipitating particles, Quart. J. Roy. Meteor. Soc. 80:522-545.

interferences in the scattered wave. The interferences in turn depend upon the wavelength of incident radiation, the size (r), index of refraction (m) of the particle, and the angular position (θ) around the scatterer. It is the relative size, that is, ratio of the particle size to wavelength (r/λ), which is the physically important parameter. At lower relative size, that is, $x \ll 1$, Mie Theory reduces to the Rayleigh approximation (Figures 6 to 8). Specifically, the Mie Theory is a mathematical series, the first terms of which are equivalent to the Rayleigh expression.[24] Thus Mie Theory describes accurately the extinction by particles of any relative size. The Mie extinction cross-section Q_{ext} and scatter cross-section Q_s are defined as

$$Q_{ext} = \frac{-\lambda^2}{2\pi} \sum_{n=1}^{\infty} (2n + 1) \, Re \, (a_n + b_n) \tag{3}$$

$$Q_s = \frac{+\lambda^2}{2\pi} \sum_{n=1}^{\infty} (2n + 1) \, [|a_n|^2 + |b_n|^2] \tag{4}$$

and from Eq. (1) the absorption cross-section Q_a is

$$Q_a = Q_{ext} - Q_s \tag{1'}$$

where a_n, b_n are the Mie coefficients

Re denotes "real part of"

The Mie coefficients are given by

$$a_n = \frac{-j_n(mx)[xj_n(x)]' - j_n(x)[mxj_n(mx)]'}{j_n(mx)[xh_n^{(2)}(x)]' - h_n^{(2)}(x)[mxj_n(mx)]'} \tag{5}$$

$$b_n = \frac{-j_n(x)[mxj_n(mx)]' - m^2 j_n(x)[xj_n(x)]'}{h_n^{(2)}(x)[mxj_n(m)]' - m^2 j_n(mx)[xh_n^{(2)}(x)]'} \tag{6}$$

---

24. Penndorf, R. (1963) Research on Aerosol Scattering in the Infrared, Final Report, AFCRL-63-688, AD

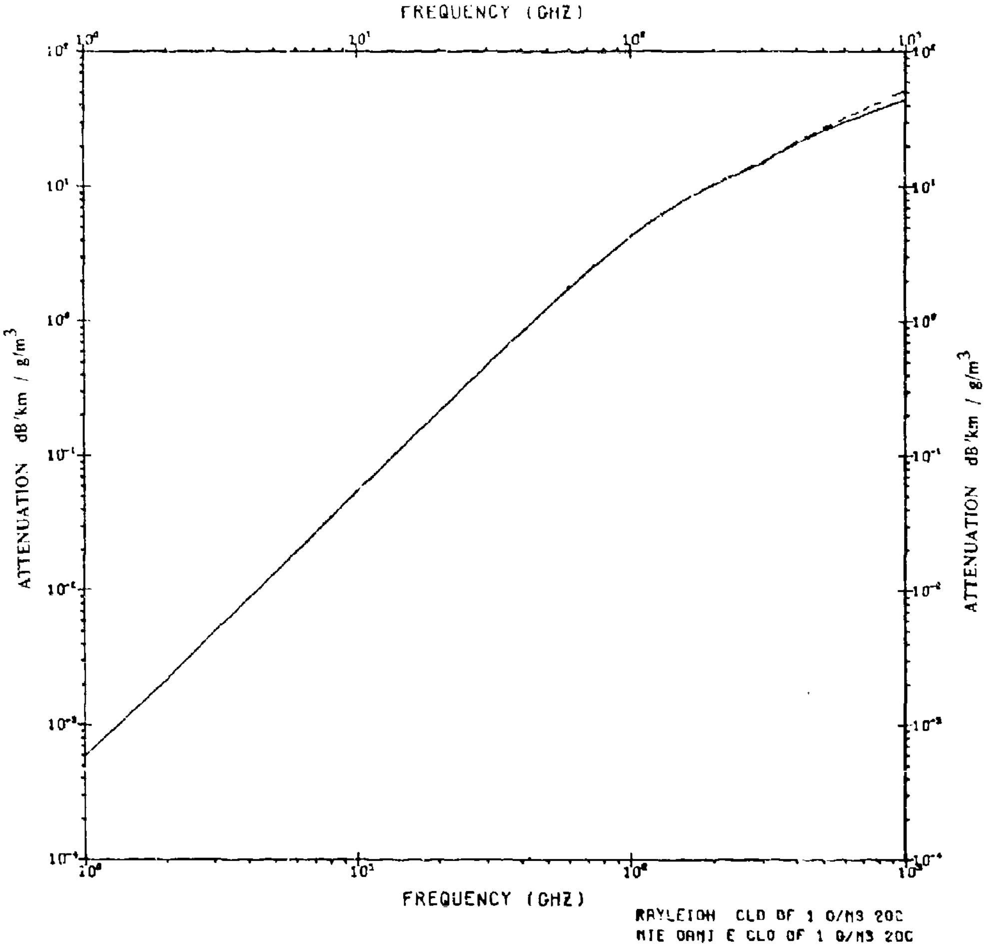

Figure 6. Comparison of the Full Mie Attenuation (dash) to Rayleigh Attenuation (solid line) vs Frequency for a Temperature of 20°C. This figure models the case which will show the largest differences (worst case)

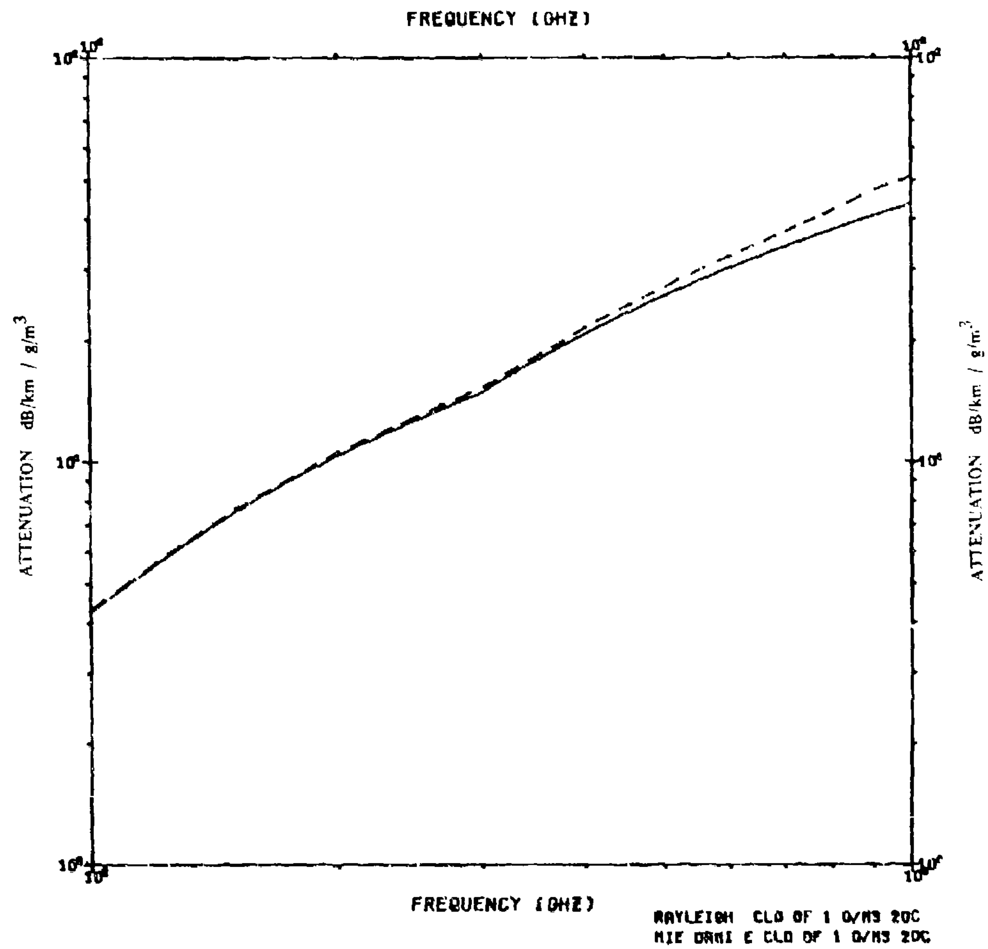

Figure 7. An Expanded Scale Comparison of Mie vs Rayleigh Attenuation. The importance of this difference between Mie and Rayleigh should be judged in view of Figure 8

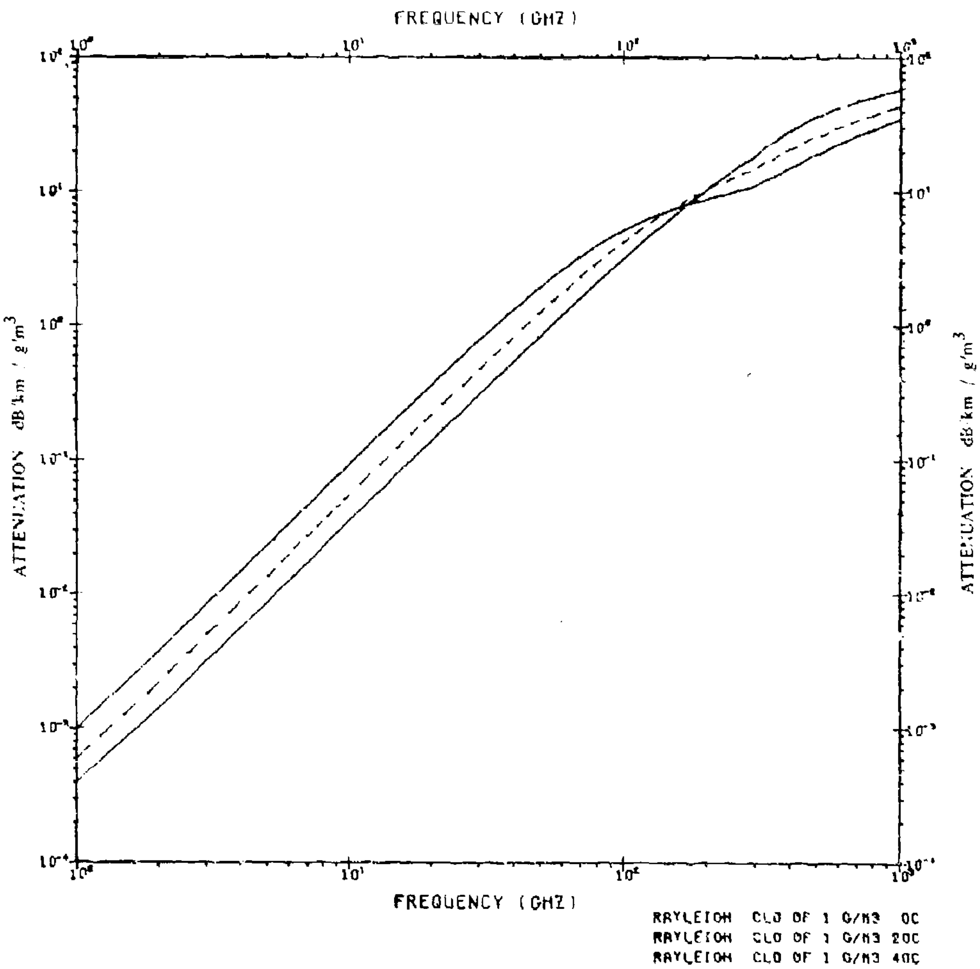

Figure 8. The Relationship of the Rayleigh Attenuation to the Temperatures 0, 20, and 40°C

where m is the complex index of refraction for the particle (drop)

' = derivative

$x = \frac{2\pi r}{\lambda}$ size parameter

r = radius of particle

j_n is n^{th} order spherical Bessel function

$h_n^{(2)}$ is n^{th} order spherical Hankel function of the second kind.

The spherical Bessel and Hankel functions are related to the ordinary cylindrical functions $j_n(x)$ and $H_n^{(2)}(x)$ by

$$j_n(x) = \left(\frac{\pi}{2x}\right)^{1/2} J_{n+1/2}(x) \quad (7)$$

$$h_n^{(2)}(x) = \left(\frac{\pi}{2x}\right)^{1/2} H_{n+1/2}^{(2)}(x) \quad (8)$$

Readers should be aware of the differences in notation between this report and works of Van de Hulst, and Deirmendjian. Van de Hulst employs an efficiency factor for extinction Q_{ext} defined as the ratio of the extinction cross-section to the geometric area presented by the drops, that is

$$Q_{ext}^{*} = \frac{Q_{ext}}{\pi r^2}$$

In Van de Hulst's notation Eq. (3) becomes

$$Q_{ext}^{*} = \frac{-2}{x^2} \sum_{n=1}^{\infty} (2n + 1) \operatorname{Re} (a_n + b_n) \quad (3')$$

Physically, the extinction cross-section efficiency factor is the fractional cross-sectional area of a particle that acts on the incident wave. Similar definitions for scattering and absorption efficiencies are defined by Van de Hulst. Deirmendjian on the other hand, uses K to represent Van de Hulst's efficiency factors. In this report $K = (m^2 - 1)/(m^2 + 2)$ (see Eqs. (10) and (11)).

In the limiting case when $r \ll 1$, that is, $x \ll 1$, the power series representation of a_n and b_n in terms of a_1, b_1 and b_2 are significant if higher terms than X^6 are neglected, see Kerr,[25] Penndorf,[24] or Van de Hulst[11] (p. 70) for details.

In this case the cross-sections reduce to the Rayleigh approximation

$$Q_{s_R} = \frac{\lambda^2}{2\pi} \frac{4}{3} x^6 \left| \frac{m^2 - 1}{m^2 + 2} \right| \quad (9)$$

25. Kerr, D.E. (Editor) (1951) Propagation of short radio waves, Radiation Laboratory Series Vol. 13, McGraw Hill, New York.

or Van de Hulst notation

$$Q^*_{s_R} = \frac{Q_{s_R}}{\pi r^2} = \frac{8}{3} x^4 \left| \frac{m^2 - 1}{m^2 + 2} \right| \qquad (9')$$

and

$$Q_{a_R} = \frac{\lambda^2}{2\pi} 2x^3 \text{ Im} \left(- \frac{m^2 - 1}{m^2 + 2} \right) \qquad (10)$$

or Van de Hulst notation

$$Q^*_{a_R} = \frac{Q_{a_R}}{\pi r^2} = 4x \text{ Im} \left(- \frac{m_2 - 1}{m^2 + 2} \right) \qquad (10')$$

where Im denotes "imaginary part of". Defining $K = (m^2 - 1)/(m^2 + 2)$, Eqs. (9) and (10) become

$$Q_{s_R} = \frac{128}{3} \pi^5 |K|^2 \frac{r^6}{\lambda^4} \qquad (11)$$

$$Q_{a_R} = 8\pi^2 \frac{r^3}{\lambda} \text{ Im } (-K) \qquad (12)$$

The complex index of refraction m is defined

$$m = n - i\kappa \qquad (13)$$

where n is the index of refraction, that is, the ratio of the speed of light in the particle to speed of light in air; κ is proportional to the bulk-absorption coefficient. Im (-K) in terms of n and κ is

$$\text{Im } (-K) = \frac{6 n\kappa}{(n^2 + \kappa^2)^2 + 4(n^2 - \kappa^2) + 4} \qquad (14)$$

Thus for a lossless dielectric, that is, one in which $\kappa = 0$, the absorption cross-section is zero. In this case the extinction (attenuation) is due entirely to scattering. This is seen by Eqs. (14), (12) and (1') where Im (-K) = 0. For a lossy dielectric as water, the absorption is appreciable. In fact, for x ≪ 1 for water, the scattering cross section is negligible in comparison with the absorption cross-section and $Q_{ext_R} \approx Q_{a_R}$. For a slightly lossy dielectric as ice, $Q_{s_R} \approx Q_{a_R}$ (not considered in this report).

The dielectric behavior of water at radio frequencies has been reported in the literature by many authors: Debye,[26] Saxton,[27] Grant,[28] and Collie.[29] The computation procedures required to quantify the real and imaginary terms of the index of refraction are such that there is disagreement among the values calculated. In order to avoid these computation differences (that is, round off errors), one computation procedure had to be chosen as a standard. In this report a paper by Ray[30] has been chosen as the standard because Ray's research covers the frequency and temperature range of interest to this report, and Ray's model is an empirical model. The complex refractive indices are calculated by the Subroutine Index given in Appendix B. Typographical errors in the tables of Ray's paper have been corrected in this subroutine.

The scattering theory discussed above is scattering from a single particle. In reality fog, clouds and rain consist of not one size particle, but many sizes. Meteorologists have studied these dropsize distributions in depth and have found them to vary with the type of fog, cloud, rain, geographical location, and season of the year. The actual dropsize distributions employed in this report are given by Silverman.[4]

Raindrop size distributions are the most complex and difficult to analyze. The distributions vary temporally and spacially within a single storm due to the effects of wind sorting (updrafts), evaporation, accretion, as well as changes in the precipitation process. The droplet distribution even differs in different parts of a single rain cloud, both vertically and horizontally.

The variation of dropsize distributions with storm type was shown by Fujiwara.[31] His results showed thunderstorms had a much wider drop size spectra than other rain, and that rain showers were intermediate between continuous rain and thunderstorms. These results are borne out by the references in Carrier.[32]

As stated previously, the distinction between clouds and rain is sometimes obscure, especially when they are mixed. Fog and clouds are assumed to be composed of water particles which are less than 100 μm in diameter. For particles this small, air currents are sufficient to overcome gravity and the particles do not fall. Clouds are generally distinguished from fog only in their distance from the earth. The fog and cloud dropsize distributions are given in many original

---

Due to the number of references to be included as footnotes on this page, the reader is referred to the list of references, page 53.

research papers. Silverman[4] summarizes both fog and cloud dropsize distributions; his table is reproduced here as Table 2 with an additional parameter, liquid water content $M(g/m^3)$. Note that the mesoscale parameter (M) liquid water content for fog and clouds are the same order of magnitude, whereas the microscale parameter of the dropsize distribution, N_0, α and b differ by orders of magnitude. On the microscale level fogs and clouds are distinguishable. This fact is important for infrared calculations of transmittance and attenuation.

Table 2. Cloud Models: Dropsize Distributions and Liquid Water Contents

$n(r) = a\, r^{\alpha} \exp[-br]$

Cloud Type	Model Number	α	b	$N_0(cm^{-3})$	a	$M(g/m^3)$
Heavy Fog 1	1	3	0.3	20	0.027	0.37
Heavy Fog 2	2	3	0.375	20	0.06592	0.19
Moderate Fog 1	3	6	1.5	100	2.37305	0.06
Moderate Fog 2	4	6	3.0	200	607.5	0.02
Cumulus	5	3	0.5	250	2.604	1.00
Altostratus	6	5	1.11	400	6.268	0.41
Stratocumulus	7	5	0.8	200	0.4369	0.55
Nimbostratus	8	1	0.333	100	11.089	0.61
Stratus	9	3	0.667	250	8.247	0.42
Stratus	10	2	0.6	250	27.00	0.29
Stratus-Stratocumulus	11	2	0.75	250	52.734	0.15
Stratocumulus	12	2	0.5	150	9.375	0.30
Nimbostratus	13	2	0.425	200	7.676	0.65
Cumulus-Cumulus Congestus	14	2	0.328	80	1.4115	0.57

Silverman's advective and radiative fog models (termed heavy fog and moderate fog respectively in this report) are in the opinion of the authors, the most representative models.[33] Advective fog is produced by the transport of moist air over a colder surface resulting in the cooling of the surface layers below their dew points, with condensation taking place in the form of fog. Most sea fogs are advective. Both the size range of particles and the liquid water contents are large (see Models 1 and 2, Table 2). Radiative fog is produced when stagnant moist air is in contact with ground that has become progressively cooler during the night due to radiative cooling. The cooling from below produces a temperature inversion in the layers next to the ground. This type of fog has both a small size range of particles and a small liquid water content (see Models 3 and 4, Table 2).

Cloud droplet size distributions are more difficult to model. Mason,[5] Fletcher,[34] and Borovikov[6] are the texts consulted by the authors. Research papers by Silverman,[4] Carrier et al,[32] and the references therein were consulted. The paper by Carrier et al was not chosen because the dropsize distributions quoted were found to be in disagreement with original references. Table 3 is our fitting of the gamma-function distribution to Carrier's Table 1.

Table 3. Dropsize Parameters for Carrier's Data

	N_o	α	$\Delta x = \frac{\Delta r}{r_{c_{mode}}}$	b	a	M g/m^3
Stratus I	464	8	0.85714	2.286	19.61	0.16
Altostratus	450	6	1.0	1.33	4.6	0.40
Stratocumulus	350	3.5	1.257	1.0	30.09	0.24
Nimbostratus	330	1.0	2.7	0.28	26.7	1.4
Fairweather C_u	300	8	0.85714	2.286	12.68	0.1
Stratus II	260	3.5	1.2667	0.777	7.182	0.37
Cumulus Congestus	207	1.5	1.914	0.4285	18.71	0.43
Cumulonimbus	72	3	1.4	0.6	1.555	0.16

33. Stewart, D.A. (1977) Infrared and Submillimeter Extinction by Fog. TR-77-9 U.S. Army Missile Research & Development, Redstone Arsenal, Alabama.

34. Fletcher, N.H. (1962) The Physics of Rain Clouds, Cambridge University Press, London.

Special notice should be given to Carrier's liquid water contents. In a private communication with Silverman, the large discrepancies between the liquid water contents calculated using a gamma function and those quoted in the literature were discussed. The values quoted by Silverman are typical clouds, based on data from Borovikov et al[6] and other sources. The variability of liquid water content may be as large as a factor of five from those quoted in Table 2. Thus, it may be seen how difficult it is to model clouds with representative dropsize spectra and liquid water content. Research has shown[35] that the liquid water content of non-precipitating clouds have values from 0.1 g/m^3-0.5 g/m^3 whereas precipitating clouds often have LWC greater than 1 g/m^3. Figures 9, 10 and 11 are dropsize distributions for fog and clouds (given by Table 2). To represent the dropsize distribution in Figures 9 to 11, Diermendjian's family of distribution functions, which he called the modified gamma function, are used

$$n(r) = a\, r^{\alpha} \exp(-br^{\gamma})\ (\mu m^{-1}\, m^{-3}) \tag{15}$$

where r is the droplet radius in units of μm and the values of α, γ are related to a and b

$$b = \frac{\alpha}{\gamma r_c^{\gamma}} \tag{16}$$

$$a = \frac{N\gamma\, b^{(\alpha+1/\gamma)}}{\Gamma(\alpha + 1/\gamma)} \tag{17}$$

where

r_c is the model radius, that is, radius of maximum concentration

Γ is the gamma function

N is the total number of particles per unit volume

$$N = \int_{r_1}^{r_2} a\, r^{\alpha} \exp(-br^{\gamma})\, dr \tag{18}$$

when $\gamma = 1$, $r_1 = 0$, $r_2 = \infty$; $N = \Gamma(r)$ thus the name modified Γ distribution.

35. Blau, H.H., Fowler, M.G., Chang, D.T. and Ryan, R.T. (1972) Cloud microstructure studies, ERT P-375 Final Report NASA Contract NAS 5-21696.

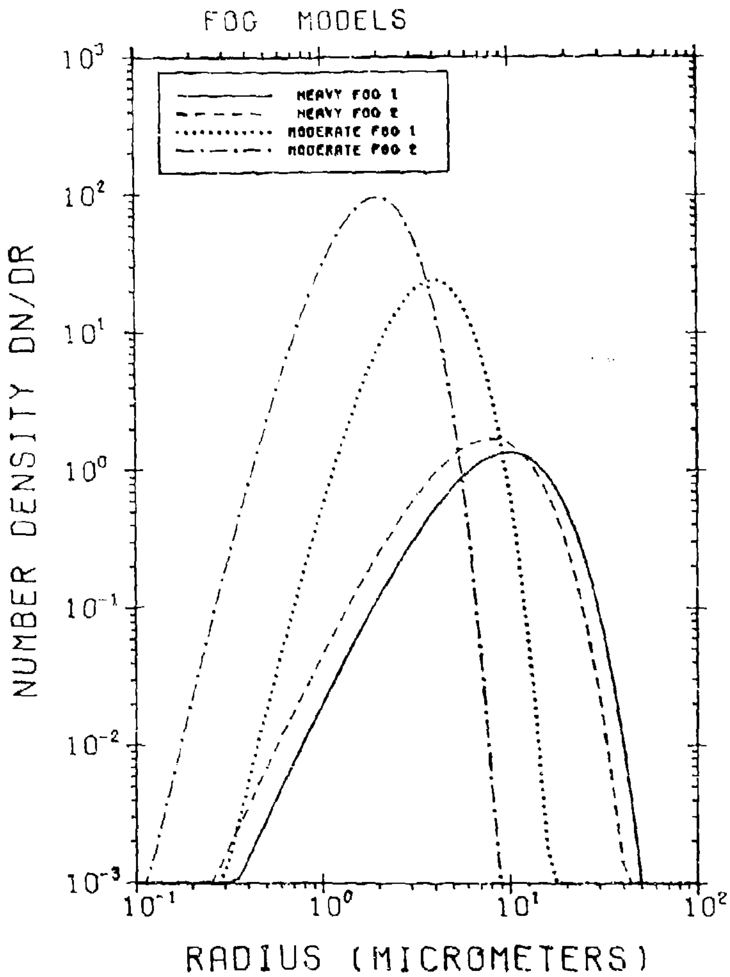

Figure 9. The Dropsize Concentration (cm^{-3} μm^{-1}) to Particle Drop Radius (μm) for Fog Models 1-4 (Table 2)

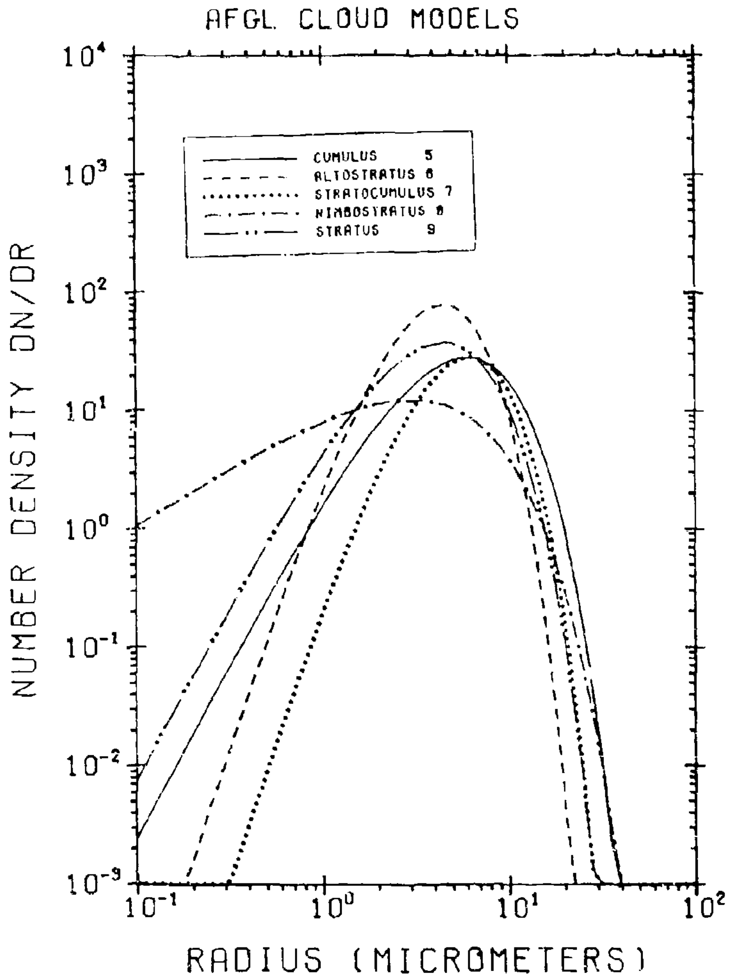

Figure 10. The Dropsize Concentration (cm^{-3} μm^{-1}) to Particle Drop Radius (μm) for Cloud Models 5-9 (Table 2)

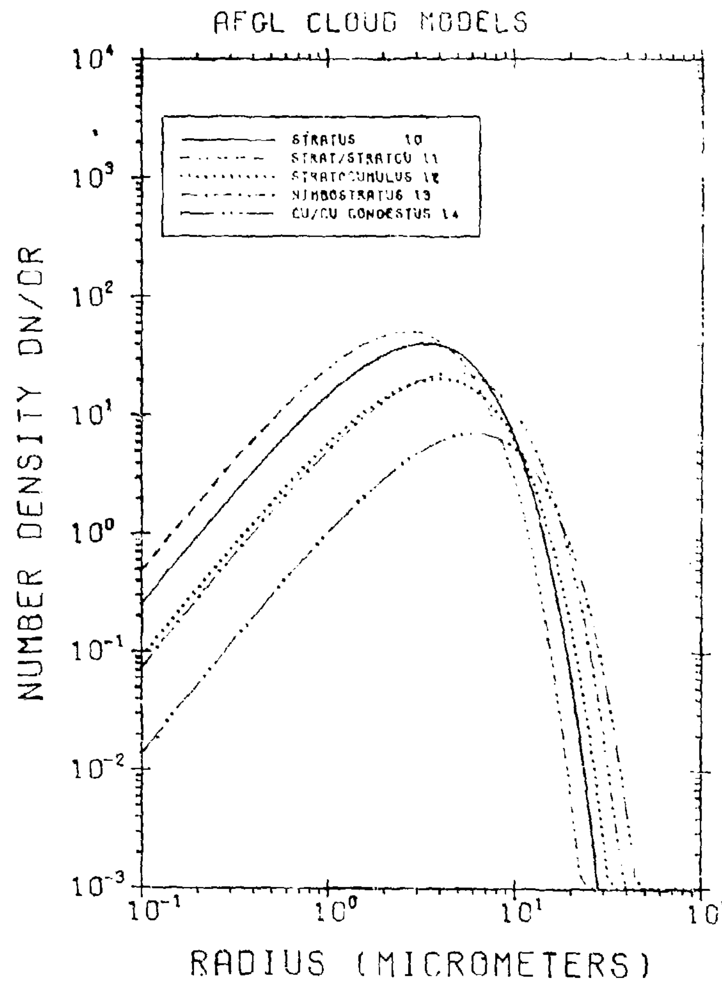

Figure 11. The Dropsize Concentration (cm^{-3} μm^{-1}) to Particle Drop Radius (μm) for Cloud Models 10-14 (Table 2)

By adjusting the four constants a, b, α and γ the modified gamma function can be adjusted to fit the various fog and cloud dropsize distributions. Tables 2 and 3 have γ set equal to 1 for computational simplicity. This follows the work of Khrgian and Mazin.[36] It should be emphasized again that the fog and clouds considered are composed of water, and water is very lossy, that is, has a relatively large imaginary component of index of refraction, so that the extinction is due to absorption only

$$Q_{a_R} \gg Q_{s_R} \Rightarrow Q_{EXT_R} \approx Q_{\ R} \quad .$$

The meteorologists usually quantify clouds by the mass of condensed water per unit of air

$$M = \frac{4}{3} \pi \rho \int_0^\infty n(r)\, r^3\, dr \ (g/m^3) \tag{19}$$

where ρ is the density of water in units of g/m^3.

Defining the volume extinction cross-section for all the particles as

$$Q_{V_{EXT}} = \int_0^\infty Q_{EXT}\, n(r)\, dr \tag{20}$$

that is, the integral of the extinction cross-section over the distribution of drops. Using Eq. (19) and Eq. (12) with ρ set equal to 1 (g/m^3), Eq. (20) becomes

$$Q_{V_{EXT}} = \frac{6\pi}{\lambda} M\, I_m(-K) \quad . \tag{21}$$

The result is that in the Rayleigh region the cloud attenuation is due to the total liquid content of the clouds. It should be emphasized again that this is true only because of the frequencies considered in this report, that is, the size parameter $x \ll 1$. The size distribution (Eq. (15)) is used to determine the liquid water content of clouds and fog via Eq. (19). As stated previously, the meteorologists quantify clouds by liquid water content (mesoscale) not dropsize distribution

36. Khrgian, A.K. and Mazin, I.P. (1956) Analysis of methods of characterizing raindrop distribution spectra, Tr. Tsents. Aerolog. Observ. Moscow (translation) 17:36-46.

(microscale). Thus the modelling efforts for clouds and fog is much simplified and the extinction calculations are just multiplications (Eq. (21)). Function GAMFOG in Appendix D accomplishes these calculations.

The calculation of attenuation (extinction) for rain requires both the full Mie series of Eq. (2) and the dropsize distribution of Eq. (15). The adaptation of Eqs. (3) through (8) to a computer is given in Deirmendjian (p. 14). This procedure has been followed. Deirmendjian also enumerates the useful properties of the modified gamma function, specifically Eqs. (16) to (18) above.

If the Deirmendjian distribution, Eq. (15), were to be used for rain calculations, the distribution function would have to be made an explicit function of rain rate, because the rain rate is the meteorologically measured parameter. This procedure of relating the modified gamma to rain rate (R) is shown by Dyer in Cole et al.[37] Another procedure would be to use Eq. (25) to relate R and the Deirmendjian distribution. In this report, rather than basing the calculations on purely mathematical (theoretical) procedures, an empirical dropsize distribution function will be used which relates n(r) to rain rate (R) explicitly.

Laws and Parsons[38] (L-P) provided the first extensive empirical data of rain rate vs dropsize distribution. Later, Marshall-Palmer[9] (M-P) proposed a dropsize distribution based on their own research and that of Laws and Parsons which has the form

$$n(D) = n_o \exp[-bD] \tag{22}$$

where

$n_o = 8 \times 10^4\ cm^{-1}\ m^{-3}$

$b = 41R^{-0.21}$

b is in units of cm^{-1}

R is rain rate ($mm\ hr^{-1}$)

D is drop diameter

Notice the original definition used drop diameter, not radius and n(D) in units of $cm^{-1}\ m^{-3}$. The units of dropsize distribution are not standardized (see Table 4). In addition weather radar specialists often use N(r) instead of n(r), however for consistency we will use n(r).

---

37. Cole, A.E., Donaldson, R.J., Dyer, R., Kantor, A.J., and Skrivanek, R.A. (1969) Precipitation and Clouds, AFCRL-69-0487.

38. Laws, J.O. and Parsons, D.A. (1943) The relation of raindrop size to intensity, Trans. Amer. Geophysical Union 24:452-460.

Table 4. Units Utilized for Scattering by Distributions

Radar Specialist	
	n(r) or n(D) in m^{-3} cm^{-1}
Weather Radar Specialists	
	n(r) or n(D) in m^{-3} mm^{-1}
Optical Specialists	
	n(r) or n(D) in m^{-3} μm^{-1}
or	
	n(r) or n(d) in cm^{-3} μm^{-1}

Meteorologists and weather radar specialists often use dropsize distribution as a function of diameter, and n(D) is either in units of cm^{-1} m^{-3} or mm^{-1} m^{-3}. Optical and infrared specialists use radius, and n(r) is in units of μm^{-1} cm^{-3}. In this report n(r) will be used witn units of mm^{-1} m^{-3}; thus Eq. (22) becomes

$$n(r) = 16000 \exp [-82R^{-0.21} r] \ mm^{-1} \ m^{-3} \qquad (23)$$

The changes in n_o and b from Eq. (22) to (23) are the result of changing from drop diameter to radius and units of cm^{-1} to mm^{-1}. Numerous other values of n_o and b have been published which allow the M-P distribution to fit measured data more accurately in varying rain (synoptic) situations (see Plank,[39] Joss[40] and Table 5 below). Other raindrop size distributions have been employed by researchers

$$n(r) = ar^{c-4} \exp (-(r/b)^3) \qquad \text{Best[41]} \qquad (24a)$$

$$n(r) = ar^3 \exp (-br) \qquad \text{Khrgian \& Mazin[36]} \qquad (24b)$$

$$n(r) = a\ r \exp (-br^{1/2}) \qquad \text{Deirmendjian[10]} \qquad (24c)$$

39. Plank, V. (1974) Hydrometeor Parameters Determined from the Radar Data of the SAMS Rain Erosion Program, AFCRL-TR-74-0249 (Environmental Research Paper No. 477), AD

40. Joss, J. and Waldwogel, A. (1969) Raindrop size distribution and sampling size errors, J. Atmos. Sci. 26:566-569.

41. Best, A.C. (1950) The size distribution of raindrops, Quart. J. Roy. Meteorol. Soc. 76:16-36.

The distributions in Eq. (24) contain several parameters which must be adjusted to fit empirical data. Unless data are available from other sources, only one parameter can be fixed. The Marshall-Palmer distribution with n_o fixed, has only one parameter b. This is another advantage of the M-P distribution over other distributions. Even though many exceptions do exist, the M-P distribution appears to be adequate (see Mason's Appendix B). It is the most representative distribution for general application, and like all the distributions given above it possesses an exponential decrease with increasing drop size. It should be mentioned that the above distributions are unimodal even though there is experimental evidence that bimodal distributions exist at high rain rates. A point specifically mentioned by many authors is that the M-P distribution overweighs the drops of very small sizes. This need not be of concern because the range of integration employed in the calculations, starts at 0.015 mm (see Table 5, section b).

Dropsize distributions are difficult to measure. What is measured is the rainfall rate (precipitation rate) R, in units of mm hr^{-1}, at ground level with rain gauges or at elevated levels by means of radar. The rain rate R is related to the dropsize distribution through the integral (see Battan[42] p. 71)

$$R = \frac{4}{3} \Pi \rho \int_{r_1}^{r_2} n(r)\, r^3 \,[v(r) - V_u]\, dr \tag{25}$$

where

R is rain rate (mm hr^{-1})

n(r) dropsize distribution (mm^{-1} cm^{-3})

r drop radius mm

v(r) terminal fall velocity of drops in (cm sec^{-1})

V_u updraft velocity (cm sec^{-1})

ρ is density of particles (liquid water density)

Physically rain rate is a flux; its units are g cm^{-2} sec^{-1} which meteorologists convert to mm hr^{-1}. In calculations it is usually assumed that $v_u = 0$ and v(r) is given empirically by Gunn and Kinzer.[43] Eq. (25) allows an internal computer check on rainfall rate used in the M-P distribution above. Employing Eq. (23) in Eq. (25) the value of n_o may be optimized for rain rates.

---

42. Battan, L. J. (1973) Radar Observations of the Atmosphere, Chicago University Press.

43. Gunn, R. and Kinzer, D. D. (1949) The terminal velocity of fall for water droplets in stagnant air, J. Meteorol. 6:243-248.

Table 5. Characteristics of Precipitation Derived from Raindrop-Size Distributions

Source	Location	Type of Precipitation	No (mm hr^{-1})	b (mm^{-1})
Marshall-Palmer	Ottawa	continuous	8,000	$4.1R^{-0.21}$
Joss	Switzerland	drizzle	30,000	$5.7R^{-0.21}$
		continuous	7,000	$4.1R^{-0.21}$
		thunderstorm	1,400	$3.0R^{-0.21}$

Joss's value of N_o = 7000 gives good results for rain rates less than 50 mm hr^{-1}. M-P continuous and Joss drizzle are used in Figure 12 to illustrate the LWC of precipitation. The range of values of r_1 and r_2 for various rain rates as given by Dyer, in Cole et al[37] are indicated in Table 6, section a. Section b values are the values used in this report.

Table 6. Range of Integration

a) Dyer		
Rain Rate (mm hr^{-1})	r_1 (mm)	r_2 (mm)
$R \leq 1$	0.33	1.13
$1 \leq R \leq 5$	0.63	1.5
$R > 25$	0.75	2.3
b) This report		
R (mm hr^{-1})	r_1 (mm)	r_2 (mm)
$.25 \leq R \leq 150$	0.015	3.3

As seen in Table 6 for the rainfall rates considered in this report, the range of integration over radius is from .015 mm to a maximum of 3.3 mm. The range of rainfall rates from 0.25 to 150 mm hr^{-1} is chosen because it is representative of rain rates encountered world wide. Rain rates as high as 300-400 mm hr^{-1} may be encountered in tropical rains, but have a time duration of only about 1 minute. Rain rates of this order are too specialized to be considered in this report, where the main emphasis is on world-wide atmospheric models.

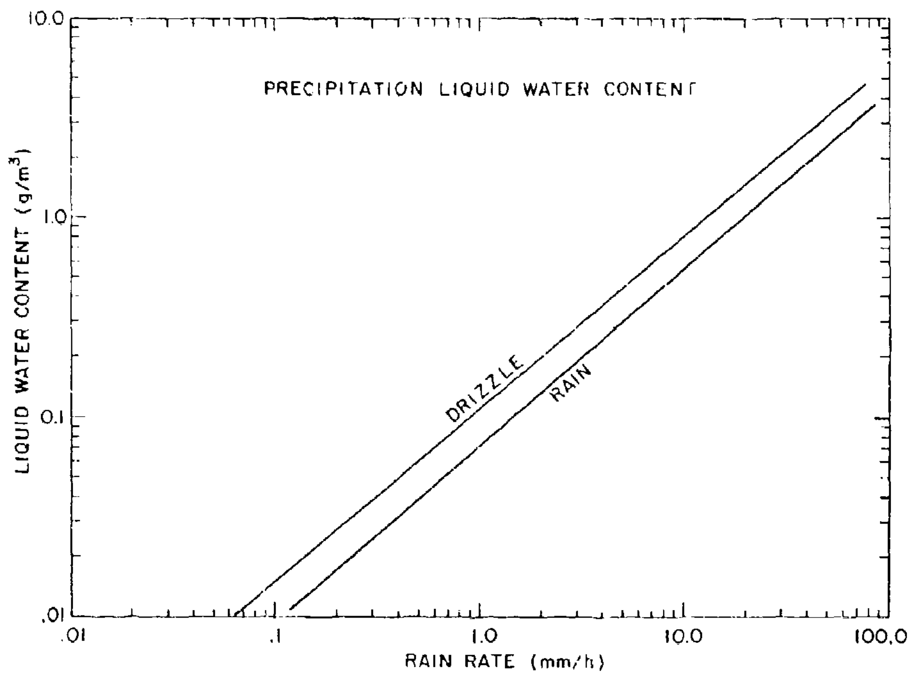

Figure 12. Liquid Water Content (g/m^3) vs a Function of Rain Rate (mm/hr) for Drizzle Employing the Joss Model for Dropsize Distribution and for Rain Employing the M-P Model. The relations are Joss $M = .11R^{.88}$; M-P $M = .072R^{.88}$

5. MODELS

This section will review typical mid-latitude fog, cloud and rain models. The general concepts for such models are given. It should be re-emphasized that the theory of scattering by hydrometeors is well known, and that the meteorological statistics of these scattering particles are not so well known. This fact impacts the systems designer of millimeter and submillimeter systems. The completely deterministic propagation system modelling of the microwave region has to be foresaken for the statistical propagation models of the millimeter and submillimeter regions forced on the system by the physical properties of the atmosphere.

In some systems the luxury of "worst case" analysis for propagation is not possible because for the worst case the atmosphere may be opaque for all practical purposes.

It is a simple procedure to identify the physical and meteorological parameters required for calculation of attenuation and transmission. They are

n(r) - dropsize distribution of hydrometeors which is related to liquid water content M and the rainfall rate R

λ - wavelength of incident electromagnetic wave

m - index of refraction of the drops

T - thermometric temperature of the drops

h - thickness of the fog, cloud, rain system

In addition it is necessary to know the frequency of occurrence of clouds, and when modelling a cloud/rain situation, it is necessary to define a consistent model of cloud liquid water content and rain.

The parameters n(r), λ, m, and T have been reviewed previously. The latter three parameters of the above list, that is, thickness h, frequency of occurrence of clouds, and a consistent water content model, will be expanded on in this section.

5.1 Cloud Models

Clouds are classified as low, middle or high according to the following rough estimates by Berry et al.[44]

low clouds	0-2000 meters
middle clouds	2000-6500 meters
high clouds	> 6500 meters

In addition to these classifications vertical development of clouds should be included. Table 7 relates the general classification of clouds to specific cloud type nomenclature.

In this report, only water clouds are considered. These clouds belong to the families of low and middle cloud classification. High clouds (cirrus) are usually composed of ice crystals. References for cloud types are Mason,[5] Borovikov,[6] Berry et al,[44] Carrier,[32] Luke,[21] Diem,[45] Weickman and Aufra Kampe,[46] Durbin,[47] Gates and Shaw,[48] and Squires and Twomey.[49]

Cloud water content is related to cloud droplet spectra by Eq. (19). Table 2 as originally proposed by Silverman is for "typical" clouds. These "typical" clouds are not average values. For example, Cloud Model 5, cumulus, has a

Due to the number of references to be included as footnotes on this page, the reader is referred to the list of references, page 53.

liquid water content of 1 g/m^3 (Table 2). This type of cloud may have typical values of liquid water from 0.5 to 1 g/m^3 with values as high as 4 g/m^3 depending on geographical location (for example, New England vs. Florida). Other types of cumulus clouds may have liquid water contents as high as 8-10 g/m^3. Liquid water content of clouds is very important to this study because the cloud droplets are Rayleigh scatterers (see Figures 6 to 8, Mie vs Rayleigh, expanded scale, and temperature dependence, respectively and Figure 13, which in addition to showing the temperature dependence of the refractive index explain the temperature cross-over of Figure 8).

The frequency of occurrence of clouds and cloud types is beyond the scope of the present paper. Systems designers and researchers should consult the following references: Solomon,[50] Guttman,[51] Quayle et al,[52] Visher,[53] and Borovikov.[6]

Table 7. Clouds Classified According to Heights

		Cloud Heights
Low Clouds		
Stratus	St	0-2000 meters
Stratocumulus	Sc	
Nimbostratus	Ns	
Middle Clouds		2000-6500 meters
Altostratus	As	
Altocumulus	Ac	
(not considered in Table 2)		
Vertical Development Clouds		
Cumulus	Cu	700-8000 meters
Cumulonimbus	Cb	700-20,000 meters
(not considered in Table 2)		

50. Solomon, I. (1963) Estimated Frequencies of Specified Cloud Amounts within Specified Ranges of Altitudes, AWS TR No. 167.

51. Guttman, N.B. (1971) Study of Worldwide Occurrence of Fog, Thundershowers, Supercooled Low Clouds and Frequency Temperatures, Navair 50-1C-60, distributed by NWSED, Asheville, N.C.

52. Quayle, R.G., Meserve, J.M. and Crutcher, H.L. (1966) Climatological Mean Probability of Penetrable Optical Path, distributed by NOAA, Asheville, N.C.

53. Visher, S.S. (1966) Climatic Atlas of the United States, Harvard University Press, Cambridge, Mass.

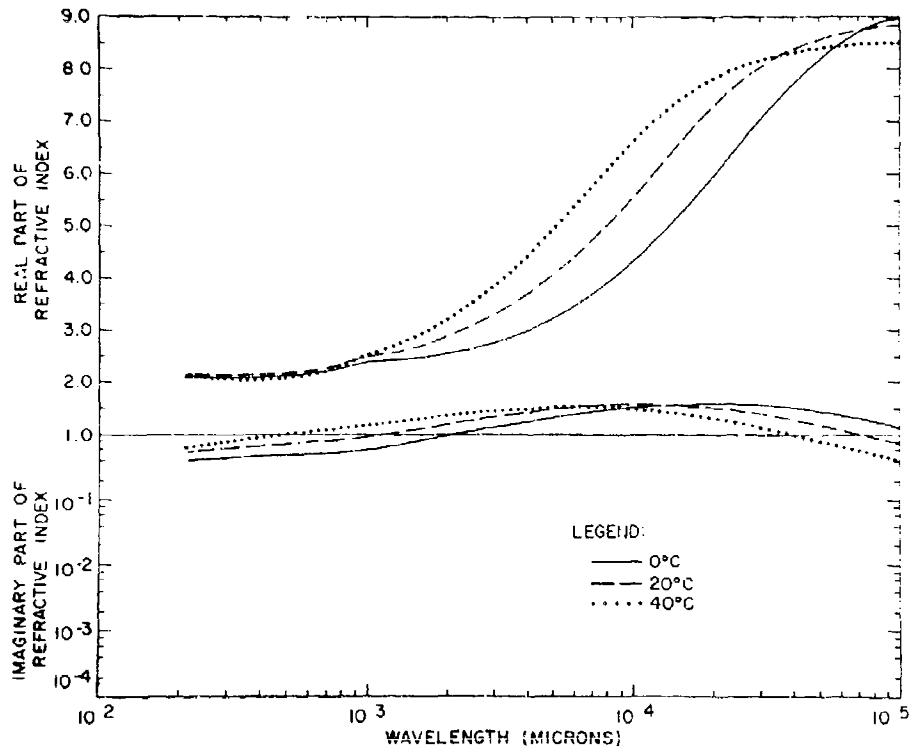

Figure 13. The Real and Imaginary Components of the Complex Dielectric Constant (Calculated from Ray) for 0°C, 20°C and 40°C

The two cloud types altocumulus and cumulonimbus of Table 7 are not considered in Table 2 because too few drop size measurements have been made in these clouds. Gates and Shaw[48] consider nimbostratus and fairweather cumulus to bracket altocumulus clouds.

In the millimeter and submillimeter frequency range, since clouds are Rayleigh scatterers, altocumulus can be modelled by assuming a liquid water content between that of the nimbostratus - and fairweather cumulus (that is, ~ 0.5 gm^{-3}).

Table 8 relates the cloud models of Table 3 to cloud thickness. The range of values of thickness may be large for these models. For example, advective fog can be from 30 meters thick to 300 meters thick depending on meteorological conditions and geographical location.

Table 8. Typical Cloud Model Thickness

Silverman's Model Number	Height (m)	
	Bottom	Top
1	0	150
2	0	150
3	0	75
4	0	75
5	660	2700
6	2400	2900
7	660	1320
8	160	1000
9	160	660
10	330	1000
11	660	2000
12	660	2000
13	160	660
14	660	2700
	660	3400

5.2 Rain Models

Precipitation as it affects propagation requires a knowledge of the variation of rainfall rate and dropsize distribution with altitude. Such data have to be related to the surface measurements of rainfall rate. The occurrence of various intensities of rainfall cannot be obtained directly from climatological records. Usually the climatological data are available for average monthly, seasonal and/or annual totals of precipitation. The quantification of rain rate (per hour) is subject to much uncertainty because rain gauge data are recorded every 6 hours. Throughout Europe and the United States clock-hourly precipitation data are available at selected weather stations. Clock-hourly rate is the total precipitation on the hour every hour. The instantaneous rates of precipitation may vary considerably within the clock-hourly rate. For example, a 0.2 mm/hr precipitation reported during a clock-hour might have accumulated in a 30 minute period at a rate of 0.4 mm/hr or in a 10 minute period at a rate of 1.2 mm/hr. Tipping bucket rain gauges may provide instantaneous rain rate; these data are available at specific weather stations. In addition to climotological data, weather radar data are available to describe the temporal and spatial range of rain rates at areas in Europe and the United States.

Two standard precipitation intensity classifications are:

1. Standard Weather Chart Code

Code	Rate (in/hr)	Rain
•	(intermittent light rain)	
••	0-01 in/hr	continuous light rain
∴	0.11-0.3 in/hr	continuous moderate rain
⁘	>0.3 in/hr	continuous heavy rain
⋮		intermittent moderate rain

Intermittent rain is not quantified in inches per hour.

2. The National Weather Service Weather Radar Code

Code	Rate (mm/hr)	Rain
0	0	none
1	0-3.8	light
2	3.8-20	moderate
3	20-40	strong
4	40-76	very strong
5	76-152	intense
6	>152	extreme

The modelling of a physically realizable cloud/rain system with altitude is extremely difficult. The model has to be consistent with respect to liquid water content (that is, the cloud associated with a specific rainfall rate must have a liquid water content the minimum value of which is of the same magnitude as the liquid water content of the precipitation). For example, the cloud associated with a 5 mm/hr surface rainfall rate must have 0.25 g/m^3 of liquid water. Water storage in clouds is another factor which has to be considered in modelling. There are three stages to a rain/cloud system, the buildup stage, the fully developed stage and the decaying stage. These stages differ in total liquid water content. We have attempted to model the fully developed stage only, that is, the models have maximum liquid water contents. The models assume maximum updrafts for maximum water storage above the cloud base. In other words these are "worst case" conditions. For applications to "typical" situations, one can safely assume the total water content of the rain/cloud system is one-half that given in the models (see Table 10). The difficulty in modelling rain/cloud systems is that the researcher does not know which stage of development the system is in unless measurements are made in real time. Also, the liquid water content can vary from 0.5 to 5 g/m^3 depending on the stage of development, season, geographical location, etc. Thus, it is obvious that only the fully developed rain/cloud stage can be successfully modelled. When applying the models, one has to keep in mind that they are "worst case" models. "Typical" models require one-half the values quoted in Table 10. In addition to the cloud liquid water content, the precipitation liquid water content beneath the cloud base has to be modelled. Table 9 relates liquid water content M (g/m^3) as a function of rain rate R (mm/hr)

Table 9. Relationship Between Liquid Water Content and Rain Rate

$M = 0.072R^{.88}$
$M = 0.07R^{.83}$
$M = 0.052R^{.97}$

Table 9 is Atlas's data taken from Sissenwine[54] and it applies to both cloud and precipitation. Other relationships have been used in which the exponent of R is set equal to 1., for example, M = 0.05R.

In addition to the liquid water of clouds and rain, the water vapor in clouds should be assumed to be at saturation (100 percent humidity).

Drizzle and orographic rain cannot be modelled as described above. The modelling of a drizzle is questionable because a drizzle is comprised of a large amount of small droplets the diameters of which are of the order of 100 μm. In this size range of particles it is difficult to separate cloud from precipitation. The drizzle for a stratus type of cloud system has a rain rate <1.25 mm/hr or a liquid water content of ~ 0.10 g/m^3 and the cloud associated with the drizzle may have LWC as high a 1 g/m^3. This associated stratus cloud may be in contact with the ground or as high as 500 m above the ground depending on the meteorological conditions. These considerations have been taken into account in the drizzle model. Drizzle Model I is a typical drizzle (see Figure 14). It is possible to model drizzle as a precipitation rate R up to the cloud base, and then a LWC in the cloud which is the sum of two equations M = 0.05R (cloud) and $M = 0.072R^{.88}$ (precipitation). These same equations have been used in Models II, III and IV (see Figures 15 through 17). Table 10 relates model altitude to liquid water content.

---

54. Sissenwine, N. (1972) Extremes of Hydrometeors at Altitude for MIL-STD-210B, AFCRL-72-0369, AD

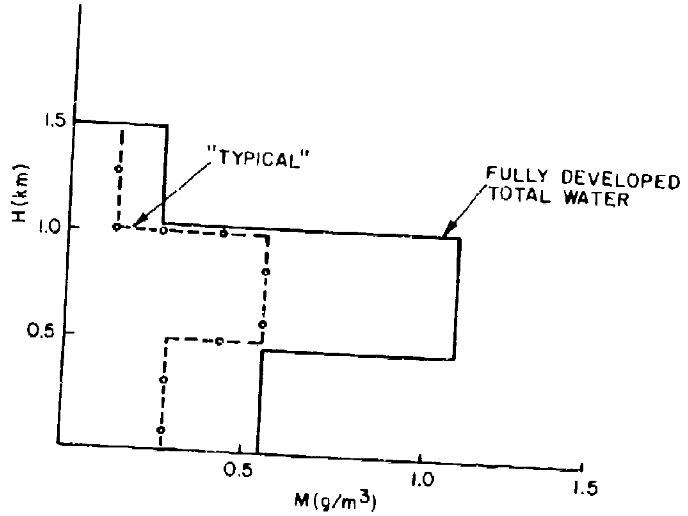

Figure 14. Model I: Drizzle, ≤1.25 mm/hr

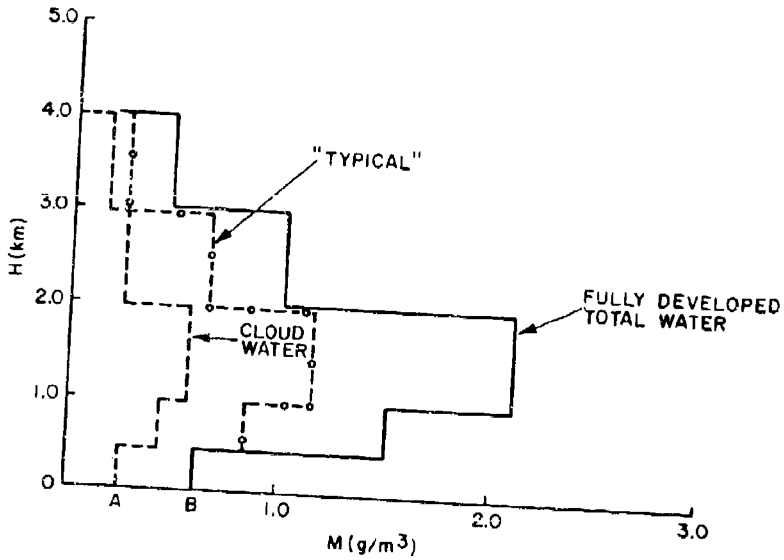

Figure 15. Model II: Steady Rain, 5 mm/hr (3-8 mm/hr)

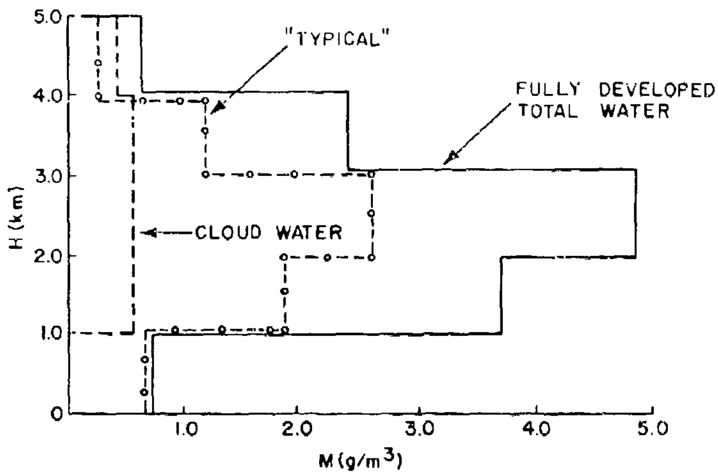

Figure 16. Model III: Steady Rain, 12.5 mm/hr (7-20 mm/hr)

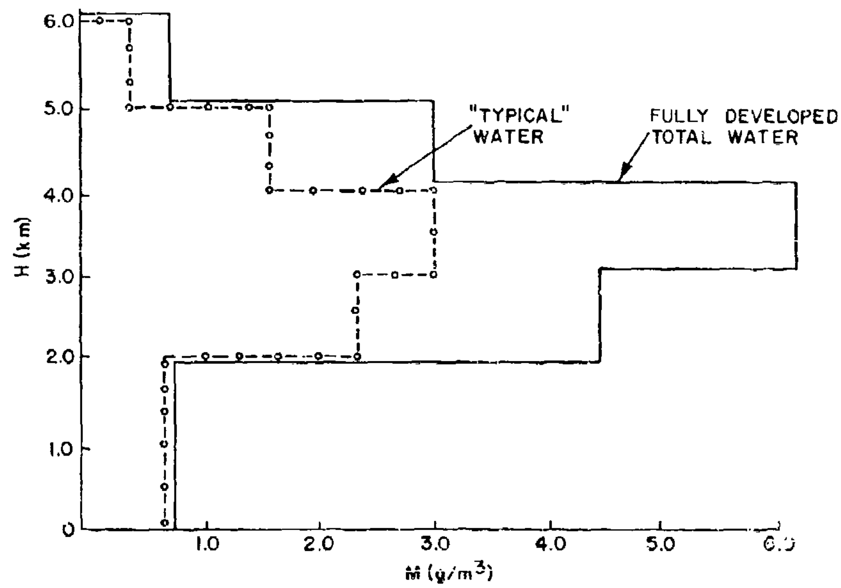

Figure 17. Model IV: Summer Cumulus, 15 mm/hr

Table 10. Rain Models

Model Name	Unit Distance (km) Base	Top	Liquid Water Content (g/m^3) Fully Developed	"Typical"
I. Drizzle	0.0	0.5	0.55	0.27
<1.25 mm/hr	0.5	1.0	1.10	0.55
	1.0	1.5	0.25	0.12
II. Steady Rain				
5 mm/hr	0.0	0.5	0.55	0.57
	0.5	1.0	1.65	0.83
3<R<8 mm/hr	1.0	2.0	2.20	1.10
	2.0	3.0	1.10	0.55
	3.0	4.0	0.30	0.15
III. Steady Rain	0.0	1.0	0.66	0.66
12.5 mm/hr	1.0	2.0	3.87	1.93
7<R<20	2.0	3.0	5.16	2.58
	3.0	4.0	2.58	1.29
	4.0	5.0	0.77	0.38
IV. Summer	0.0	2.0	0.80	0.80
Cumulus	2.0	3.0	4.65	2.32
15 mm/hr	3.0	4.0	6.20	3.10
	4.0	5.0	3.10	1.55
	5.0	6.0	0.93	0.46

The Models II, III, and IV as given in Table 10 have been generated from data of Valley[3] and the research of Wexler and Atlas,[55] East,[56] Kessler,[57] Langille and Gunn,[58] and Hamilton.[59] In order to derive general concepts (rules-of-thumb) to model rain, the research of the above authors has been compared with the M-P formula and the cloud liquid water content formulae. The factors required to multiply the M-P formula and the cloud LWC formula are given in the following steps:

---

55. Wexler, R. and Atlas, D. (1958) Moisture supply and growth of stratiform precipitation, J. Meteor. 15:531-539.

56. East, T.W.R. (1957) An inherent precipitation mechanism in cumulus clouds, Quart. J. R. Met. Soc. 83:61-69.

57. Kessler, R. (1961) Kinimatical relations between wind and precipitation distributions II, J. Meteor. 18:510-.

58. Langille, R.C. and Gunn K. L. S. (1948) Quantitative analysis of vertical Structure in precipitation, J. Meteor. 5:310-.

59. Hamilton, P.M. (1966) Vertical profiles of total precipitations in shower situations, Quart. J. Roy. Meteor. Soc. 92:346-362.

1. The liquid water content of the cloud is expressed by the formula

$$M\ (g/m^3) = 0.05R$$

N.B. for R < 8 mm/hr the cloud (d < 100 μm) may touch the earth's surface, as in Model II. For higher rain rates (R) this is not true (see Model III); at these higher rain rates the larger drops scavenge the smaller droplets.

2. At the cloud base the sum of the LWC of the rain and the cloud is multiplied by a factor of 3 for a unit altitude. For Model I the unit altitudes are all 0.5 km. For Model II the first unit altitude is 0.5 km and subsequent unit altitudes are 1 km. For Model III the unit altitude is 1.0 km. For Model IV, a summer cumulus rain, the cloud base is raised to 2 km and the cloud top to 6 km.

3. At an altitude of one unit distance above the cloud base the LWC of the rain plus cloud is multiplied by 4, the next unit distance the LWC is multiplied by 2 and the last unit distance the LWC is multiplied by 0.5.

Figure 18 is an example of the attenuation over a 1 kilometer horizontal path through clear, cloudy and rainy atmosphere.

It should be emphasized that the above models are to be used only as examples of typical rain/cloud models. The computer program given in Appendix D can be used to model any real meteorological system. It is the responsibility of the researcher to determine what is a realistic model for the geographical location being considered.

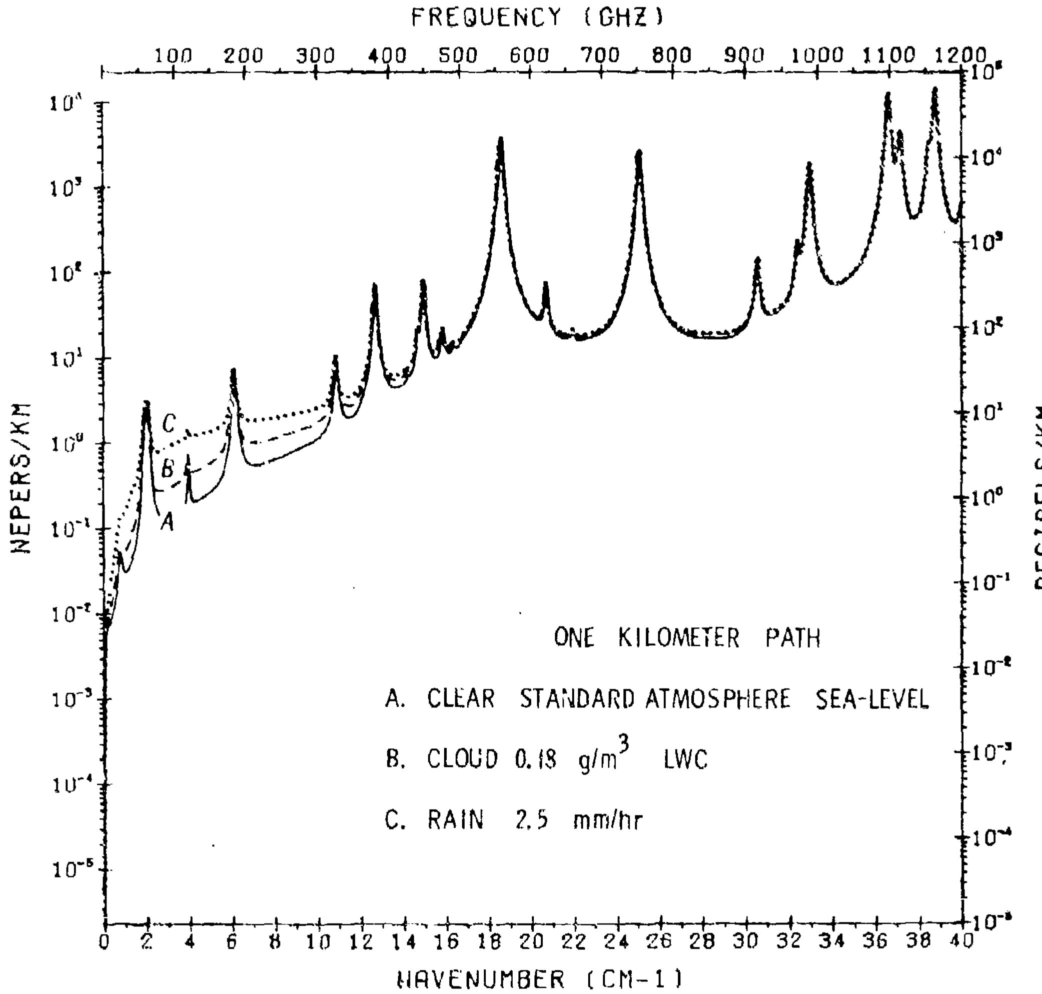

Figure 18. Attenuation vs Frequency for a Clear Standard Atmosphere, a Cloud of 0.18 g/m^3 LWC, and a 2.5 mm/hr Rain Rate for a 1 Kilometer Horizontal Path

References

1. McClatchey, R.A., Fenn, R.W., Selby, J., Volz, F.E., and Garing, J.S. (1972) Optical Properties of the Atmosphere (3rd Ed.), AFCRL-72-0497, AD 753 075.

2. Selby, J.E.A. and McClatchey, R.A. (1972) Atmospheric Transmission From 0.25 to 28.3 um: Computer Code LOWTRAN 2, AFCRL-72-0745, AD 763 721.

3. Valley, S.L. (Editor) (1965) Handbook of Geophysics and Space Environments, AFCRL.

4. Silverman, B.A. and Sprague, E.D. (1970) Airborne Measurements of In-Cloud Visibility, National Conference on Weather Modification of the American Meteorological Society, April 6-9, Santa Barbara, California.

5. Mason, B.J. (1971) The Physics of Clouds, Clarendon Press, Oxford.

6. Borovikov, A.M., Khrgian, A.K.H. and others (1963) Cloud physics, U.S Department of Commerce, Office of Technical Services.

7. McClatchey, R.A., Benedict, W.S., Clough, S.A., Burch, D.E., Calfee, R.F., Fox, K., Rothman, L.S. and Garing, J.S. (1973) AFCRL Atmospheric Absorption Line Parameters Compilation, AFCRL-TR-73-0096, AD 762 904.

8. Clough, S.A. et al. (1980) FASCOD-1, AFGL Technical Report, to be published.

9. Marshall, J.S. and Palmer, W.M.K. (1948) The distribution of raindrops with size, J. Meteor. 5:165-166.

10. Deirmendjian, D. (1969) Electromagnetic Scattering on Polydispersions, Elsevier Publishing Co.

11. Van DeHulst, H.C. (1957) Light Scattering by Small Particles, John Wiley & Sons Inc.

12. Kerker, M. (1969) The Scattering of Light and Other Electro-Magnetic Radiation, Academic Press.

13. Oguchi, T. (1973) Attenuation and phase rotation of radio waves due to rain: calculations at 19.3 and 34.8 GHz, Radio Science Vol. 8:31-38.

14. Hogg, D.C. (1969) Statistics on attenuation of microwaves in intense rain, Bell System Technical Journal Vol. 48:2949-2963.

15. Rider, G.C. (1966) Propagation measurements of "Q" band rainfall attenuation, Marconi Revue Vol. 29:24-30.

16. Norbury, J.R. and White, W.J.K. (1972) Microwave attenuation at 35.8 GHz due to rainfall, Electronics Letters Vol. 8 No. 4:91-92.

17. Robinson, N.P. (1955) Measurements of the Effect of Rain, Snow and Fogs on 8.6 mm Radar Echoes, Proc. I.E.E. London, Vol. 102B:709-714.

18. Mueller, G.E. (1946) Propagation of 6-millimeter waves, Proc. IRE Vol. 34:181P-183P.

19. Jones, D.M.A. (1959) The shape of raindrops, J. Meteor. 16:504-510.

20. Oguchi, T. (1960) (1964) Attenuation of electromagnetic wave due to rain with distorted raindrops, J. Radio Res. Lab. (Japan) 7:467, Part II, J. Radio Res. Lab. 11:19.

21. Luke, G.D. (1968) Penetrability of haze, fog, clouds and precipitation by radiant energy over the spectral range 0.1 micron to 10 centimeters, NAVWAG Study 61, AD 847658, Maj.

22. Mie, G. (1908) Beitrage zur optik truber medien, speziell kollodaler metallosungen, Ann der Phys. 25:377-445.

23. Gunn, K.L.S. and East, T.W.R. (1954) The microwave properties of precipitating particles, Quart. J. Roy. Meteor. Soc. 80:522-545.

24. Penndorf, R. (1963) Research on Aerosol Scattering in the Infrared, Final Report, AFCRL-63-688.

25. Kerr, D.E. (Editor) (1951) Propagation of short radio waves, Radiation Laboratory Series Vol. 13, McGraw Hill, New York.

26. Debye, P. (1929) Polar Molecules, Dover Press, New York.

27. Saxton, J.A. (1946) The anamolous supervision of water at very high radio frequencies, Meteorological Factors in Radio-Wave Propagation, The Physical Society, London, 293-328.

28. Grant, E.H., Buchanan, T.J., and Cook, H.F. (1957) Dielectric behavior of water at microwave frequencies, J. Chem. Phys. 26, No. 1:156-.

29. Collie, C.H., Hastel, J.B., and Ritson, D.M. (1948) The cavity resonator method of measuring the dielectric constant of polar liquids, Pro. Phys. Soc. London, 60:71-82.

30. Ray, P.S. (1972) Broadband complex refractive indices of ice and water, App. Opt. 11:1836-1844.

31. Fujiwara, M. (1965) Raindrop-size distribution from individual storms, J. Atmosp. Sci. 22:585-591.

32. Carrier, L.W., Cato, G.A., and von Essen, K.J. (1967) The backscatter and extinction of visible and infrared radiation by selected major cloud models, App. Optics 6:1209-1216.

33. Stewart, D.A. (1977) Infrared and Submillimeter Extinction by Fog, TR-77-9 U.S. Army Missile Research & Development, Redstone Arsenal, Alabama.

34. Fletcher, N.H. (1962) The Physics of Rain Clouds, Cambridge University Press, London.

35. Blau, H.H., Fowler, M.G., Chang, D.T., and Ryan, R.T. (1972) Cloud microstructure studies, ERT P-375 Final Report NASA Contract NAS 5-21696.

36. Kirgian, A.K. and Mazin, I.P. (1956) Analysis of methods of characterizing raindrop distribution spectra, Tr. Tsents. Aerolog. Observ. Moscow (translation) 17:36-46.

37. Cole, A.E., Donaldson, R.J., Dyer, R., Kantor, A.J., and Skrivanek, R.A. (1969) Precipitation and Clouds, AFCRL-69-0487, AD 703 288.

38. Laws, J.O. and Parsons, D.A. (1943) The relation of raindrop size to intensity, Trans. Amer. Geophysical Union 24:452-460.

39. Plank, V. (1974) Hydrometeor Parameters Determined from the Radar Data of the SAMS Rain Erosion Program, AFCRL-TR-74-0249 (Environmental Research Paper No. 477), AD 786 454.

40. Joss, J. and Waldwogel, A. (1969) Raindrop size distribution and sampling size errors, J. Atmos. Sci. 26:566-569.

41. Best, A.C. (1950) The size distribution of raindrops, Quart. J. Roy. Meteorol. Soc. 76:16-36.

42. Battan, L.J. (1973) Radar Observations of the Atmosphere, Chicago University Press.

43. Gunn, R. and Kinzer, D.D. (1949) The terminal velocity of fall for water droplets in stagnant air, J. Meteorol. 6:243-248.

44. Berry, F.A., Bollary, E., and Beers, N.R. (1945) Handbook of Meteorology, Chapter 11, McGraw Hill.

45. Diem, M. (1948) Messurngen der grosser von wolkenelementen II, Meteorologisete Rundeschen 9/10:261-273.

46. Weickman, H.K. and Aufra Kampe, H.J. (1953) Physical properties of cumulus clouds, J. Meteor. 10:204-211.

47. Durbin, W. (1959) Droplet sampling in cumulus clouds, Tellus 7:202-215.

48. Gates, D. and Shaw, C. (1960) Infrared transmission of clouds, J. Opt. Soc. Am. 50:876-882.

49. Squires, P. and Twomey, S. (1960) The relation between cloud droplet spectra and the spectrum of cloud nuclei, Amer. Geophys. Uni. 15:211-219.

50. Solomon, I. (1963) Estimated Frequencies of Specified Cloud Amounts within Specified Ranges of Altitudes, AWS TR No. 167.

51. Guttman, N.B. (1971) Study of Worldwide Occurrence of Fog, Thundershowers, Supercooled Low Clouds and Frequency Temperatures, Navair 50-1C-60, distributed by NWSED, Asheville, N.C.

52. Quayle, R.G., Meserve, J.M., and Crutcher, H.L. (1966) Climatological Mean Probability of Penetrable Optical Path, distributed by NOAA, Asheville, N.C.

53. Visher, S.S. (1966) Climatic Atlas of the United States, Harvard University Press, Cambridge, Mass.

54. Sissenwine, N. (1972) Extremes of Hydrometeors at Altitude for MIL-STD-210B, AFCRL-72-0369, AD 747 482.

55. Wexler, R. and Atlas, D. (1958) Moisture supply and growth of stratiform precipitation, J. Meteor. 15:531-539.

56. East, T.W.R. (1957) An inherent precipitation mechanism in cumulus clouds, Quart. J. R. Met. Soc. 83:61-69.

57. Kessler, E. (1961) Kinematical relations between wind and precipitation distributions II, J. Meteor. 18:510-.

58. Langille, R.C. and Gunn, K.L.S. (1948) Quantitative analysis of vertical structure in precipitation, J. Meteor. 5:310-.

59. Hamilton, P.M. (1966) Vertical profiles of total precipitations in shower situations, Quart. J. Roy. Meteor. Soc. 92:346-362.

Bibliography

Anderson, W.E. (1970) Characteristics of Clouds, Honeywell, Roseville, Minn., SRSD-41.

Babkin, Yu.S., et al. (1970) Attenuation of radiation at a wavelength of 0.96 mm in snow, Rad. Eng. and Elec. Phys. Vol. 15:2171-2174.

Babkin, Yu.S., et al. (1970) Measurement of attenuation in rain over 1 km path at a wavelength of 0.96 mm, Rad. Eng. and Elec. Phys. Vol. 15:2164-2166.

Blevis, B.C. (1974) Microwave attenuation and scatter theory and measurement, J. de Richerches Atmosphereques Vol. 8:5-21.

Blevis, B.C., Dohoo, R.M., McCormick, K.S. (1967) Measurements of rainfall attenuation at 8 and 15 GHz, Trans. Ante and Prop. Vol. AP-15:394-403.

Byers, R.H. (1965) Elements of Cloud Physics, University of Chicago Press, Chicago.

Chen, C.C. (1975) Attenuation of Electromagnetic Radiation by Haze, Fog, Clouds and Rain, Rand Corporation Report R-1694-PR.

Chu, T.S. (1974) Rain-induced cross-polarization at centimeter and millimeter wavelengths, Bell System Tech. J. Vol. 53:1557-1579.

Chu, T.S. and Hogg, D.C. (1968) Effects of precipitation on propagation at 0.63, 3.5 and 10.6 microns BSTJ, May-June:723-759.

Crane, R.K. (1966) Microwave Scattering Parameters of New England Rain, Lincoln Laboratory Technical Report 426 (ESD-TR-66-447).

deBettencourt, J.T. (1974) Statistics of millimeter-wave rainfall attenuation, J. de Recherches Atmosphereque Vol. 8:89-119.

Donaldson, R.J. (1961) Radar Reflectivity Profiles in Thunderstorms, J. Met. Vol. 18:292-

Fedi, F. et al. (1974) Attenuation: theory and measurements, J. de Recherches Atmosphereques Vol. 8:465-472.

Fowler, M.G., Hardy, K.R., Dak Sze, N. (1976) The Development of a Model to Infer Precipitation from Microwave Measurements, ERT Final Report, NASA Contract NA-20868.

Gant, N.E., Reiffenstein, E.C., Chang, D.T. (1972) Microwave Properties of the Atmosphere, Clouds and the Ocean, ERT Final Report NASA Contract NAS-5-21624.

Haan, Mei-Yuan (19) Microstructure of cumulus clouds, Isv. Geophys. Ser. No. 2:362-376.

Hogg, D.C. and Chu, T S. (1975) The role of rain in satellite communications, Proc. IEEE, Vol. 63:1308-1331.

Krasyuk, N.P., Rogenberg, V.I., Chistyakov, D.A. (1968) Attenuation and Scattering of Radio Synols by Rain with Shufrin and Marshall-Palmer Drop Size Distribution, Rad. Eng. and Elec. Phys. Vol. 13:1638-1640.

Medhurst, R.G. (1965) Rainfall attenuation of centimeter waves: comparison of theory and measurement, IEEE Trans. Ant. & Prop. AP-13:550-564.

Olsen, R.L., Rogers, D.V., and Hodge, D.B. (1978) The aR^b relation in the calculation of rain attenuation, IEEE Trans. Antennas Propagat. Vol. AP-26: 318-329.

Pruppacher, H.R., Klett, J.D. (1978) Microphysics of Clouds and Precipitation, D. Resdel Pub. Co., Holland.

Pruppacher, H.R. and Pitte, R.L. (1971) A semi-empirical determination of the shape of cloud and rain drops, J. Atm. Scies. Vol. 28:86-94.

Rogers, D.V. and Olsen, R.L. (1976) Calculation of Radiowave Attenuation Due to Rain at Frequencies up to 1000 GHz, CRC Report 1299.

Sander, J. (1975) Rain attenuation of millimeter waves at $\lambda = 5.77$, 3.3 and 2 mm, Trans. Ant. and Prop. Vol. AP-23:213-220.

Savage, R.C. (1978) The radiation properties of hydrometeors at microwave frequencies, J. of Appl. Meteor. Vol. 17:904-911.

Shisno, J. (1978) A numerical study of precipitation development in cumulus clouds, Papers in Meteorology and Geophysics Vol. 29:157-193.

Sokolov, A.V. (1970) Attenuation of visible and infrared radiation in rain and snow, Rad. Eng. and Elec. Phys. Vol. 15:2175-2178.

Sokolov, H.V., Sukhonin, Ye.V. (1970) Attenuation of submillimeter radio waves in rain, Radio Eng. and Elec. Physics, Vol. 15:2167-2171.

Warner, J. (19) The microstructure of cumulus clouds, Part II: the effect on droplet size distribution of cloud nucleus spectrum and updraft velocity, J. Atmos. Science 26:1272-1282.

World Meteorological Organization (1956) International Cloud Atlas, Geneva, Switzerland.

Appendix A

Definitions

a) Transmittance and attenuation

As stated in the text, the AFGL line-by-line absorption calculation code HITRAN, was generated by infrared specialists. These specialists use transmittance to characterize atmospheric propagation, whereas, microwave specialists use attenuation to characterize the same atmospheric propagation. The attenuation (α) is related to transmittance (τ) by the formula

$$\alpha = 1 - \tau$$

The transmittance at a single frequency for a path of length x is

$$\tau = \frac{\text{emergent power}}{\text{incident power}} = I/I_o$$

For optical on IR propagation, the rate of attenuation is generally given as an attenuation coefficient, β, which is expressed as the fractional reduction in the transmitted energy per unit length along the direction of propagation

$$\beta = \left(\frac{dI}{I}\right)/dx = \frac{\ln \tau}{x}$$

so the units are reciprocal length (here km^{-1})

b) Decibels and Nepers

For microwave and radio propagation the attenuation is generally given in terms of a decibel (dB) or neper (less commonly) loss. Decibels are defined by:

$$\text{number of decibels} = 10 \log_{10} \left(\frac{I}{I_o}\right) = 10 \log_{10} \tau$$

A 1 neper attenuation means a reduction to 1/e of the original value* or number of nepers = ln (I/I_o) = (number of decibels)/4.343

$$\beta(\text{km}^{-1}) = \beta(\text{neper/km}) = \beta(\text{db/km})/4.343$$

Optical depths are dimensionless. It should be kept in mind that both nepers (logarithms to base e) or decibels (logarithms to base 10) are dimensionless units and the two are related by,

$$1\text{Np} = 10 \text{ Log}_{10} \text{ e dB} = 4.343 \text{ dB}$$

---

*It should be noted that neper loss is frequently applied to the voltage or amplitude of the electromagnetic signal on wave and not to the transmitted energy on power, as we use above. This leads to an extra factor of 2 relating nepers to decibels.

1 neper reduction in amplitude = 8.686 decibel reduction in intensity

Appendix B

Subroutine AERSOL

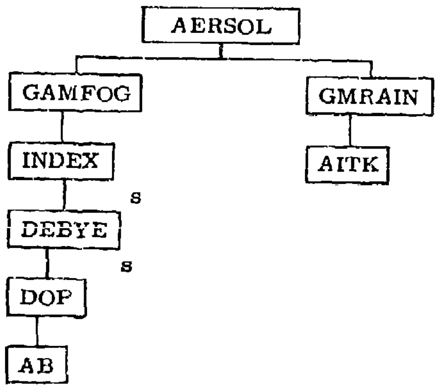

FUNCTION GAMFOG calculates attenuation due to fog/cloud liquid water content (g/m^3) by the equation

$$\gamma_F = 8.1888 \frac{1}{\lambda} M \, \mathrm{Im}\left(-\frac{m^2 - 1}{m^2 + 2}\right)$$

where λ = wavelength in cm

M = liquid water content (g/m^3)

m = complex index of refraction calculated in subroutine INDEX

FUNCTION GMRAIN - calculates extinction due to rain by the full Mie theory, as a function of wavelength temperature, and drop-size.

- drop-size distribution is Marshall-Palmer

$n(r) = N_o \text{ EXP } (-br)$

- DATA WVLTAB	is wavelength table used in ATTAB
- DATA ATTAB	is attenuation data table in dB/km for temperature 20°C Table B1 (abridged version)
- DATA TMPTAB	is interpolation data table for temperatures in °K Table B2
- DATA TLMDA	is interpolation data table for wavelength in cm
- DATA RATTAB	is rain rate table in mm/hr

Subroutine INDEX

Applied Optics vol 11 No. 8 Aug. 1972 pp 1836-1844

Typographic errors in original paper have been corrected as follows:

pg 1837 $\lambda \geq 3000\ \mu$, $\epsilon' = 2(t + 273)/5 + 72$

should be

$\lambda \geq 300$ cm , $\epsilon' = 2T/5 + 88$

pg 1840 - Table 11 Δ_i column sixth from top 0.08 should be 0.009

- equation 12 d. 10^{-4} should be 10^{-5}

Table 111 - w_{o_i} column fifth from top 688.24 should be 588.24

- Equation $n(r) = n_r^a (7.0 - \lambda) + n_r^b (\lambda - 6\lambda)$

should be $n(r) = n_r^a (7.0 - \lambda) + n_r^b (\lambda - 6)$

Table B1. Attenuation (db/km) at 20^{o}C Wavelength (cm)

PRECIPITATION RATE (MM/HR)	.03	.05	.1	.15	.2	.25	.3	.5	.8	1.0	2.0	3.0	5.0	6.0	15.0
0.25	.867	.900	.874	.77[illegible]	.656	.539	.434	.179	.0634	.0381	.685 x10^{-2}	.231 x10^{-2}	.657 x10^{-3}	.434 x10^{-3}	.631 x10^{-4}
1.25	2.31	2.43	2.51	2.41	2.22	1.99	1.74	.919	.374	.232	.0449	.0134	.104 x10^{-2}	.191 x10^{-2}	.249 x10^{-3}
2.50	3.51	3.71	3.90	3.83	3.63	3.34	3.01	1.77	.783	.497	.104	.0311	.618 x10^{-2}	.374 x10^{-2}	.454 x10^{-3}
5.00	5.35	5.65	6.01	6.02	5.83	5.49	5.08	3.29	1.60	1.05	.239	.0750	.0132	.758 x10^{-2}	.829 x10^{-3}
12.50	9.35	9.86	10.59	10.80	10.69	10.33	9.81	7.13	3.94	2.70	.698	.245	.0399	.0209	.186 x10^{-2}
25.00	14.27	15.03	16.18	16.67	16.70	16.38	15.81	12.36	7.51	5.38	1.52	.591	.100	.0488	.348 x10^{-2}
50.00	21.78	22.90	24.68	25.61	25.89	25.70	25.14	20.89	13.87	10.37	3.23	1.38	.265	.124	.661 x10^{-2}
100.00	33.22	34.85	37.55	39.18	39.84	39.96	39.50	34.54	24.83	19.40	6.66	3.09	.706	.338	.0128
150.00	42.48	44.51	47.93	50.16	51.10	51.54	51.22	45.94	34.46	27.59	10.06	4.86	1.24	.613	.0190

Table B2. Temperature Correction Factor for Representative Rains

PRECIPITATION RATE MM/HR	WAVELENGTH CM	0°	10°	20°	30°	40°
	.03	1.0	1.0	1.0	1.0	1.0
	.1	0.99	0.99	1.0	1.01	1.02
0.25	.5	1.02	1.01	1.0	1.0	1.0
	1.25	1.05	1.02	1.0	1.0	0.99
	3.2	1.55	1.25	1.0	0.81	0.65
	10.0	1.72	1.29	1.0	0.79	0.64
	.03	1.0	1.0	1.0	1.0	1.0
	.1	1.0	1.0	1.0	1.0	1.01
2.5	.5	1.01	1.01	1.0	0.99	0.98
	1.25	0.95	0.96	1.0	1.05	1.10
	3.2	1.28	1.14	1.0	0.86	0.72
	10.0	1.73	1.30	1.0	0.79	0.64
	.03	1.0	1.0	1.0	1.0	1.0
	.1	1.0	1.0	1.0	1.0	1.01
12.5	.5	1.02	1.01	1.0	0.99	0.97
	1.25	0.96	0.97	1.0	1.04	1.07
	3.2	1.04	1.03	1.0	0.95	0.88
	10.0	1.74	1.30	1.0	0.79	0.63
	.03	1.0	1.0	1.0	1.0	1.0
	.1	1.0	1.0	1.0	1.0	1.01
50.0	.5	1.02	1.01	1.0	0.98	0.97
	1.25	0.99	0.99	1.0	1.02	1.04
	3.2	0.91	0.96	1.0	1.01	1.01
	10.0	1.75	1.31	1.0	0.78	0.62
	.03	1.0	1.0	1.0	1.0	1.0
	.1	1.0	1.0	1.0	1.0	1.01
150.0	.5	1.03	1.01	1.0	0.98	0.97
	1.25	1.01	1.0	1.0	1.0	1.01
	3.2	0.88	0.95	1.0	1.04	1.06
	10.0	1.72	1.31	1.0	0.78	0.62

Appendix C

Computer Input Instructions

Programs required: FASCOD1, HIRAC1, LBLF4, SCANFN1, FCODMRG and the subroutine package AERSOL.

To utilize the Aerosol Subroutine in calculation of Attenuation in the Microwave region (1-1000 GHz) the input control cards must be as follows:

*5.1 CARD 1: XID(I), I=1, 7)
FORMAT (10A10)

AN IDENTIFICATION CHOSEN BY THE USER TO BE PRINTED AT THE START OF THE OUTPUT AND AS A HEADER FOR ANY PLOTTED FILE.

5.2 CARD 2: IHIRAC, ILBLF4, ICNTNM, IAERSL, IEMIT, ISCAN, IPLOT, MPTS, NPTS
FORMAT (7I5, 35X, 3I5)

IHIRAC = 1 CALL HIRAC1
VAN VLECK-WEISSKOPF APPROXIMATION TO LINE SHAPE USED IN MICROWAVE REGION

IHIRAC = 2 CALL HIRACL
LORENTZ APPROXIMATION TO LINE SHAPE

IRIRAC = 3 CALL HIRACD
DOPPLER APPROXIMATION TO LINE SHAPE

*The description of input control cards 1-7 is brief and accurate at the present time. For a detailed and up-to-date description see FASCODE1 Report by Clough et al.[8]

ILBLF4(0, 1) Flag for LBLF4 (LINE BY LINE FUNCTION 4)

1 = Yes (extends calculation to 256 $\bar{\alpha}_v$)

ICNTNM = 0, 1 Flag for continuum (CONTNM)

1 = Yes

IAERSL = 0 No AERSOL Calculations

= 1 AERSOL Calculations desired

(MUST FOLLOW INPUT OF AERSOL DATA AS EXPLAINED IN SECTION 5.9)

IEMIT = 0 No Emission - Only Attenuation (Absorption Coefficient)

= 1 Emission and Transmission calculations performed

ISCAN (0, 1) Flag for SCANFN 1 = Yes

IPLOT (0, 1) Flag for PLOT 1 = Yes

MPTS = 0 Number of points to be printed from panel

NPTS = 1-20

Controls number of output data points to be printed from merge routines.

5.3 CARD 3: V1, V2 (cm^{-1})

FORMAT (2E10.3)

Beginning and ending wave number values for the calculations.

5.4 CARD 4: TBOUND (^{o}K)

FORMAT (E10.3)

Boundary temperature (for ICNTRL=1 CASE only)

5.5 CARD 5: ANGLE (degrees)

FORMAT (E10.3)

Secant angle as measured from local zenith. Calculation performed for Angle of 0^{o}-60^{o} and ANGLE of 120^{o}-180^{o}

0^{o}-60^{o} sets control (ICNTRL=3) for looking up case

120^{o}-180^{o} sets control (ICNTRL=1) for looking down case

otherwise secant = 0, and ICNTRL=0.

IF ANGLE NOT IN THESE RANGES - SECANT AND ICNTRL WILL BE READ FROM LAYER CARD (see card 7)

5.6 CARD 6: NLAYRS

FORMAT (I5)

NUMBER OF LAYERS INPUT

5.7 CARD 7: PAVE, TAVE, SECNTK, ICNTRK, (FILHD(I), I=1, 4)

FORMAT (3F10.4, I5, 4A10)

PAVE: Average pressure (MB) for the layer

TAVE: Average temperature (^{o}K) for the layer

SECNTK: A non zero value for SECNTK will override the value calculated from Angle.

ICNTRK - IF ≠ 0 It replaces value of ICNTRL

= 1, Looking from H1 toward H2 for H1 > H2

= 2, Looking from H1 toward H2 for H1 = H2

= 3, Looking from H1 toward H2 for H1 < H2

(FILHD(I), I=1, 4): Descriptive text defining beginning and ending of layer in (KM) (Col. 36-75)

5.8 CARD 8: (WK(M), M=1, 7)

FORMAT (7E10.3)

WK: Array containing the molecular densities for the layer in (Molecules/cm^2)

for: H_2O, CO_2, O_3, N_2O, CO, CH_4, O_2

5.9 After each input layer of CARD 7 and CARD 8 and etc. The following procedure must be followed in order to utilize the Aersol calculations.

5.9.1 CARD 9: NLYRS

FORMAT (I5, 2F10.3)

NLYRS: Must be 1 less than number of cld, fog, and or rain cards read in.

NLYRS = Blank or Ø: signifies no cloud, fog, and or rain between that particular layer.

5.9.2 CARDS 10-NN: Where NN is 11-29

The maximum number of input CLOUD, FOG, and or RAIN data cards between each main program layer is 20. If more are needed than change the dimensions of RRA, HDIF, T2 and C2 in subroutine AERSOL as desired:

H, P, T, RH, CLOUD, RAIN

FORMAT (F5.1, 5F10.3)

H: Height of Layer in KM

P: Pressure for that Height in MB

T: Temperature in (°K)

RH: Relative Humidity values of 0 → 1.0

CLOUD: Liquid water content of cloud or fog in (g/m^3)

RAIN: Rainfall rate in (MM/HR)

5.10 Example of card squencing for a specific case.

Problem: Calculate Absorption Coefficient for three 2 KM layers with clouds and rain in the first 4 KM for 0-40 (cm^{-1}) wavenumbers.

(* REPRESENTS A SPACE ON THE CARD)

Layer	Card	Content
	CARD 1:	FASCODE MICRO WAVE REGION TEST
	CARD 2:	****1****1****1****1****0
	CARD 3:	***0.0********40.0
	CARD 4:	BLANK
	CARD 5:	*****0.0
	CARD 6:	****3
1st Layer	CARD 7:	**903.25**281.7624********************0.0KM to 2.0KM
	CARD 8:	2.825E+22*1.517E+21*1.355E+12*1.287E+18 *3.448E+17*7.357+18*9.632E+23*3.590E+24
	CARD 9:	***4
	CARD 10:	**0.0****1013.3*****291.2*******1.0*****0.000 ********2.00
	CARD 11:	**0.5*****954.6*****288.9*******1.0*****0.015 ********1.91
	CARD 12:	**1.0*****898.8*****286.7*******1.0*****0.045 ********1.78
	CARD 13:	**1.5*****845.6*****284.3*******1.0*****0.078 ********1.61
	CARD 14:	**2.0*****795.0*****282.2*******1.0*****0.106 ********1.43
2nd Layer	CARD 15:	**705.0873**268.3198********************2.0KM to 4.0KM
	CARD 16:	*1.24[illegible]E+22*1.245E+21*1.252E+17*1.056E+18 *2.828E+17*6.034E18*7.901E+23*2.945E+24
	CARD 17:	****4
	CARD 18:	**2.0***** 795.0*****282.2*******1.0*****0.106 ********1.43
	CARD 19:	**2.5*****746.9*****279.8*******1.0*****0.134 ********1.25
	CARD 20:	**3.0*****701.2*****277.7*******1.0*****0.158 ********1.06
	CARD 21:	**3.5*****657.8*****275.3*******1.0*****0.176 ********0.87
	CARD 22:	**4.0*****616.6*****273.2*******1.0*****0.160 ********0.70
3rd Layer	CARD 23:	**543.7893**255.8787********************4.0KM to 60KM
	CARD 24:	*4.531E+21*1.010E+21*1.142E+17*8.568E+17 *2.295E+17*4.896E+18,6.411E+23*2.390E+24
	CARD 25:	blank (no rain and or cloud this layer)

LAST CARD: *.0001********0.0******40.0

Appendix D

Listing of Program

```
      SUBROUTINE AERSOL(IRAD)
C * * ****************************************************************
C * *
C * *    PROGRAM AERSOL
C * *
C * *  CALCULATES ATTENUATION IN THE MICROWAVE,MILLIMETER
C * *  AND SUB-MILLIMETER REGIONS
C * *
C * *          1 MAR 1979
C * *
C * *
C * *      AUTHORS
C * *
C * *     LEONARD W. ABREU  A.F.G.L.   617-861-4775
C * *
C * *     VINCENT J. FALCONE   A.F.G.L.   AUTOVON  478-4775
C * *
C * * ****************************************************************
      COMMON /ABSORP/V1D,V2D,DVD,NPTD,D(205)
      COMMON /FILHDR/ XID(10),SECANT,PAVE,TAVE,HMCLID(20),WK(20),WN2,DV,
     1V1,V2,TBOUND,FSCDID(17),NMOL,NLAYER
      DIMENSION DPF(205),RRA(20),HDIF(20)
      DIMENSION T2(20),C2(20)
CCC   NLYRS MUST BE 1 LESS THAN NUMBER OF CLD AND OR RAIN CARDS INPUT
CCC   BETWEEN EACH LAYER READ IN FROM MAIN PROGRAM.
CCC   BLANK CARD READ IN - SIGNIFIES NO RAIN AND OR CLD DATA BETWEEN
CCC   THAT PARTICULAR LAYER.
CCC   FROM THE SECOND LAYER ON IT IS NECESSARY TO REPEAT THE PREVIOUS
CCC   TOP LEVEL INPUT.
CCC   EG.  INPUT AFTER MAIN PROGRAM LAYER OF 0-2KM IS
CCC   2                =NLYRS
CCC   0.0 KM   ETC. . .
CCC   1.0 KM   ETC. . .
CCC   2.0 KM   ETC. . .
CCC   THEN INPUT AFTER MAIN PROGRAM LAYER OF 2-4 KM IS
CCC   2                =NLYRS
CCC   2.0 KM   ETC. . .
CCC   3.0 KM   ETC. . .
CCC   4.0 KM   ETC. . .
CCC   MAXIMUM NUMBER OF INPUT CLD AND OR RAIN LAYERS BETWEEN EACH
CCC   MAIN PROGRAM LAYER IS 20.
      READ 915,NLYRS
      IF(NLYRS.NE.0) GO TO 98
      RETURN
   98 CONTINUE
      TP=0.0
      CP=0.0
      READ 910,H,P,T,RH,CLOUD,RAIN
      PRINT 919,H,P,T,RH,CLOUD,RAIN
      OLDT=T
      OLDH=H
      FIRSTH=H
      OLDC=CLOUD
      OLDR=RAIN
      PRINT 918
      DO 110 L=1,NLYRS
      READ 910,H,P,T,RH,CLOUD,RAIN
```

```
      PRINT 919,H,P,T,RH,CLOUD,RAIN
      HDIF(L)=H-OLDH
      RRA(L)=(OLDR+RAIN)/2.
      T2(L)=(OLDT+T)/2.
      C2(L)=(OLDC+CLOUD)/2.
      C2(L)=C2(L)*HDIF(L)
      TP=TP+T2(L)*C2(L)
      CP=CP+C2(L)
      PRINT 924,OLDH,H,T2(L),C2(L),RRA(L)
      OLDT=T
      OLDH=H
      OLDC=CLOUD
      OLDR=RAIN
  119 CONTINUE
      FINALH=H
      PRINT 916,FIRSTH,FINALH
      FIRSTH=H
      TAV=TP/CP
      BETA=1.0/(0.6951*TAV)
      CALL SECOND(X0)
      DO 201 J=2,NPTD
      VJ=V10+FLOAT(J-1)*DVD
      GJ=VJ*29.97925
      GMRANT=0.0
      GAMCLD=0.0
      DO 120 L=1,NLYRS
      GAMCLD=GAMCLD+GAMFOG(GJ,T2(L),C2(L))
      GMRANT=GMRANT+HDIF(L)*GMRAIN(GJ,T2(L),RRA(L))
  120 CONTINUE
      DJ=GMRANT/4.343+GAMCLD/4.343
      DRF(J)=DJ
      EXPVJ=EXP(-VJ*BETA)
      RADFAC=VJ*(1.-EXPVJ)/(1.+EXPVJ)
      IF(J.EQ.2) D2=DJ/RADFAC
      IF(J.EQ.3) D3=DJ/RADFAC
      D(J)=D(J)+DJ/RADFAC
  201 CONTINUE
      CALL SECOND(X1)
      TIME=X1-X0
      D(1)=D(1)+D2-(D3-D2)
      PRINT 915,TIME
      PRINT 917,V10,V20
      PRINT 920,(D(J),J=1,NPTD)
  301 CONTINUE
  905 FORMAT(I5,2F10.3)
  910 FORMAT(F5.1,5F10.3)
  915 FORMAT(10X,* TIME=*,F10.5/)
  916 FORMAT(1H1,10X,*HGT=*,F5.1,* TO *,F5.1//)
  917 FORMAT(15X,*V10=*,F10.3,*V20=*,F10.3//5X,*D(J),J=1,NPTD   RAIN + CL
     1OUD*//)
  918 FORMAT(1H1,5X,* INPUT DATA AVG TEMP AND AVG CLOUD LYRS*//)
  919 FORMAT(//10X,F5.1,5F10.3//)
  920 FORMAT(5X,10E12.5)
  924 FORMAT(10X,* OLDH=*,F5.1,* H=*,F5.1,* T2=*,F10.3,* C2=*,F10.3,
     1* RRA=*,F10.3/)
      RETURN
      END
```

```
      SUBROUTINE INDEX(WAVL,TC,KEY,REAL,AIMAG)
C * * * * * * * * * * * * * * * * * * * * * * * * * * * * * * * * * *
C * *
C * * WAVELENGTH IS IN CENTIMETERS.  TEMPERATURE IS IN DEG. C.      * *
C * *
C * * KEY IS SET TO 1 IN SUBROUTINE GAMFOG                          * *
C * *
C * * REAL IS THE REAL PART OF THE REFRACTIVE INDEX.               * *
C * *
C * * AIMAG IS THE IMAGINARY PART OF THE REFRACTIVE INDEX IT IS    * *
C * *
C * * RETURNED NEG. I.E.  M= REAL - I*AIMAG  .                       * *
C * *
C * * A SERIES OF CHECKS ARE MADE AND WARNINGS GIVEN.               * *
C * *
C * * RAY APPLIED OPTICS VOL 11,NO.8,AUG 72, PG. 1836-1844          * *
C * *
C * * CORRECTIONS HAVE BEEN MADE TO RAYS ORIGINAL PAPER             * *
C * *
C * *
C * * * * * * * * * * * * * * * * * * * * * * * * * * * * * * * * * *
      R1=0.0
      R2=0.0
      IF(WAVL.LT..0001) WRITE(6,1)
      IF(TC.LT.-20.) WRITE(6,2)
    1 FORMAT(///,30X,*ATTEMPTING TO EVALUATE FOR A WAVELENGTH LESS THAN
     1ONE MICRON*,//)
    2 FORMAT(///,30X,*ATTEMPTING TO EVALUATE FOR A TEMPERATURE LESS THAN
     2 -20. DEGREES CENTIGRADE*,//)
      CALL DEBYE(WAVL,TC,KEY,REAL,AIMAG)
C * *  TABLE 3 WATER PG. 1840
    4 IF(WAVL.GT..034) 5,7
    5 IF(WAVL.GT..1) 11,6
    6 R2 =DOP(WAVL,1.83899,1639.,52340.4,10399.2,586.24,345005.,
     3259913.,161.29,43319.7,27661.2)
      R2=R2+R2*(TC-25.)*.0001*EXP((.000025*WAVL)**.25)
      REAL=REAL*(WAVL-.034)/.066+R2*(.1-WAVL)/.066
      GO TO 11
    7 IF(WAVL.GT..0006) 8,10
    8 REAL=DOP(WAVL,1.83899,1639.,52340.4,10399.2,588.24,345005.,
     4259913.,161.29,43319.7,27661.2)
      REAL=REAL+REAL*(TC-25.)*.0001*EXP((.000025*WAVL)**.25)
      IF(WAVL.GT..0007) 11,9
    9 R1=DOP(WAVL,1.79907,3352.27,99.914E+04,15.1963E+04,1639.,50483.5,
     59246.27,588.24,84.4697E+04,10.7615E+05)
      R1=R1+R1*(TC-25.)*.0001*EXP((.000025*WAVL)**.25)
      REAL=R1*(.0007-WAVL)/.0001+REAL*(WAVL-.0006)/.0001
      GO TO 11
   10 REAL=DOP(WAVL,1.79907,3352.27,99.914E+04,15.1963E+04,1639.,
     650483.5,9246.27,588.24,84.4697E+04,10.7615E+05)
      REAL=REAL+REAL*(TC-25.)*.0001*EXP((.000025*WAVL)**.25)
C * *  TABLE 2 WATER PG. 1840
   11 IF(WAVL.GE..3) GO TO 57
      IF(WAVL.GE..03) 12,13
   12 AIMAG=AIMAG+AB(WAVL,.25,300.,.47,3.)+AB(WAVL,.39,17.,.45,1.3)+
     7AB(WAVL,.41,62.,.35,1.7)
      GO TO 57
```

```
  SUBROUTINE INDEX       74/74    OPT=1                              FTN 4.6+460       0

         13 IF(WAVL.GE..0062) 14,15
         14 AIMAG=AIMAG+AB(WAVL,.41,62.,.35,1.7)+AB(WAVL,.39,17.,.45,1.3)+
           8AB(WAVL,.25,300.,.4,2.)
            GO TO 57
         15 IF(WAVL.GE..0017) 16,17
         16 AIMAG=AIMAG+AB(WAVL,.39,17.,.45,1.3)+AB(WAVL,.41,62.,.22,1.8)+
           9AB(WAVL,.25,300.,.4,2.)
            GO TO 57
         17 IF(WAVL.GE..00061) 18,19
         18 AIMAG=AIMAG+AB(WAVL,.12,6.1,.042,.6)+AB(WAVL,.39,17.,.165,2.47+
           1AB(WAVL,.41,62.,.22,1.8)
            GO TO 57
         19 IF(WAVL.GE..000495) 20,21
         20 AIMAG=AIMAG+AB(WAVL,.01,4.95,.05,1.)+AB(WAVL,.12,6.1,.009,2.)
            GO TO 57
         21 IF(WAVL.GE..000297) 22,23
         22 AIMAG=AIMAG+AB(WAVL,.27,2.97,.04,2.)+AB(WAVL,.01,4.95,.06,1.)
            GO TO 57
         23 AIMAG=AIMAG+AB(WAVL,.27,2.97,.025,2.)+AB(WAVL,.01,4.95,.06,1.)
         57 CONTINUE
            RETURN
            END
```

```
  SUBROUTINE DEBYE       74/74    OPT=1                              FTN 4.6+460       0

            SUBROUTINE DEBYE(WAVL,TC,KEY,RE,AI)
            T=TC+273.
            IF(KEY.NE.0) 1,2
          1 EFIN=5.27137+.0216474*TC-.00131198*TC*TC
            ALPHA=-16.8129/T+.0609265
            TAU=.0003836*EXP(2513.98/T)
            SIG=12.5664E+08
            ES=78.54*(1.-.004579*(TC-25.)+.0000119*(TC-25.)**2-.000000028*
           1(TC-25.)**3)
            GO TO 3
          2 EFIN=3.168
            ALPHA=.00023*TC*TC+.0052*TC+.288
            SIG=1.26*EXP(-12500./(T*1.9869))
            TAU=9.990288E-05*EXP(13200./(T*1.9869))
            ES=3.168+.15*TC*TC+2.5*TC+200.
          3 C1=TAU/WAVL
            C2=1.5708*ALPHA
            DEM=1.+2.*C1**(1.-ALPHA)*SIN(C2)+C1**(2.*(1.-ALPHA))
            E1=EFIN+(ES-EFIN)*(1.+(C1**(1.-ALPHA)*SIN(C2)))/DEM
            IF(KEY.NE.0.AND.WAVL.GE.300.) E1=2.*TC/5.+88.
            E2=(ES-EFIN)*C1**(1.-ALPHA)*COS(C2)/DEM+SIG*WAVL/18.8496E+10
            RE=SQRT((E1+SQRT(E1*E1+E2*E2))/2.)
            AI=-E2/(2.*RE)
            RETURN
            END
```

FUNCTION DOP 74774 OPT=1 FTN 4.6+460

```
      FUNCTION DOP(WAVL,A,CEN1,B,C,CEN2,D,E,CEN3,F,G)
      V=1./WAVL
      V2=V*V
      H1=CEN1**2-V2
      H2=CEN2**2-V2
      H3=CEN3**2-V2
      DOP=SQRT(A+B*H1/(H1*H1+C*V2)+D*H2/(H2*H2+E*V2)+F*H3/(H3*H3+G*V2))
      RETURN
      END
```

FUNCTION AB 74774 OPT=1 FTN 4.6+460

```
      FUNCTION AB(WAVL,A,CEN,B,C)
      AB=-A*EXP(-ABS((ALOG10(10000.*WAVL/CEN)/B))**C)
      RETURN
      END
```

FUNCTION GAMFOG 74774 OPT=1 FTN 4.6+460

```
      FUNCTION GAMFOG(FRQG,T,RHO)
C
C        COMPUTES ATTENUATION OF CONDENSED WATER IN CLOUDS OR FOG
C
C        FRQG  = FREQUENCY (GHZ)
C        FREQ  = WAVENUMBER (INVERSE CM)
C        T     = TEMPERATURE (DEGREES KELVIN)
C        RHO   = CONDENSED WATER VAPOR CONTENT  (G/CUBIC METER)
C     CINDEX=COMPLEX DIELECTRIC CONSTANT M  FROM INDEX
C
      COMPLEX CINDEX,CINDX
      IF(RHO.GT.0.) GO TO 2
      GAMFOG=0.
      RETURN
    2 FREQ=FRQG/29.979
      KEY=1
      WAVL=29.979/FRQG
      TC=T-273.2
      CALL INDEX(WAVL,TC,KEY,REAL,AIMAK)
      CINDEX=CMPLX(REAL,AIMAK)
      GAMFOG=8.1888*FREQ*RHO*AIMAG( -  (CINDEX**2-1)/(CINDEX**2+2))
      RETURN
      END
```

```
      FUNCTION AITK(ARG,VAL,X,NDIM)
C
C      IBM SCIENTIFIC SUBROUTINE
C
C
      DIMENSION ARG(NDIM),VAL(NDIM)
      IF(NDIM-1)9,7,1
C
C     START OF AITKEN-LOOP
    1 DO 6 J=2,NDIM
      IEND=J-1
      DO 2 I=1,IEND
      H=ARG(I)-ARG(J)
      IF(H)2,13,2
    2 VAL(J)=(VAL(I)*(X-ARG(J))-VAL(J)*(X-ARG(I)))/H
    6 CONTINUE
C     END OF AITKEN-LOOP
C
    7 J=NDIM
    8 AITK=VAL(J)
    9 RETURN
C
C     THERE ARE TWO IDENTICAL ARGUMENT VALUES IN VECTOR ARG
   13 IER=3
      J=IEND
      GO TO 8
      END
```

```
      FUNCTION GMRAIN(FREQ,T,RATE)
C
C        COMPUTES ATTENUATION OF CONDENSED WATER IN FORM OF RAIN
C
C        FREQ = FREQUENCY (GHZ)
C        T    = TEMPERATURE (DEGREES KELVIN)
C        RATE = PRECIPITATION RATE (MM/HR)
C
C
C     TABLES ATTAB AND FACTOR CALCULATED FROM FULL MIE THEORY
C     UTILIZING MARSHALL-PALMER SIZE DISTRIBUTION WITH RAYS INDEX
C     OF REFRACTION
C
C     ATTAB IS ATTENUATION DATA TABLE IN DB/KM FOR 20 DEG CELSIUS
C
C     WVLTAB IS WAVELENGTH TABLE FOR WAVELENGTHS USED IN TABLE ATTAB
C
C     TMPTAB IS INTERPOLATION DATA TABLE FOR TEMPERATURES IN DEG KELVIN
C
C     TLMDA IS INTERPOLATION DATA TABLE FOR WAVELENGTH IN CM
C
C     RATTAB IS RAIN RATE TABLE IN MM/HR
C
C     FACTOR IS TABLE OF TEMPERATURE CORRECTION FACTORS FOR
C     TABLE ATTAB FOR REPRESENTATIVE RAINS
C
C
C     AITKEN INTERPOLATION SCHEME WRITTEN BY
C           F.T. FLORANCE O.N.R. PASADENA CA.
C
C
      DIMENSION ATTAB(27,9),WVLTAB(27),RATTAB(9),FACTOR(5,6,5)
      DIMENSION X(3),Y(3),ATTN(3),RATES(3)
      DIMENSION TMPTAB(5),TLMDA(6),FACIT(5),TFACT(5)
      DATA WVLTAB/.03,.033,.0375,.043,.05,.06,.075,.1,.15,.2,.25,.3,.5,
     1.8,1.,2.,3.,4.,5.,5.5,6.,6.5,7.,8.,9.,10.,15./
      DATA RATTAB /.25,1.25,2.5,5.,12.5,25.,50.,100.,150./
      DATA TLMDA/.03,.1,.5,1.25,3.2,10./
      DATA TMPTAB/273.,283.,293.,303.,313./
      DATA(ATTAB(I,1),I=1,27)/.867,.875,.884,.893,.900,.902,.899,
     1.874,.773,.656,.539,.434,.179,.0634,
     2.0381,.685E-2,.231E-2,.112E-2,.657E-3,.528E-3,.434E-3,
     3.363E-3,.309E-3,.232E-3,.180E-3,.145E-3,.631E-4/
      DATA(ATTAB(I,2),I=1,27)/2.31,2.33,2.36,2.39,2.43,2.46,2.50,
     12.51,2.41,2.22,1.99,1.74,.919,.374,
     2.232,.0449,.0134,.563E-2,.304E-2,.234E-2,.191E-2,
     3.157E-2,.132E-2,.967E-3,.741E-3,.588E-3,.249E-3/
      DATA(ATTAB(I,3),I=1,27)/3.51,3.55,3.60,3.65,3.71,3.77,3.84,
     13.90,3.83,3.63,3.34,3.01,1.77,.783,
     2.497,.104,.0311,.0122,.618E-2,.473E-2,.374E-2,
     3.304E-2,.252E-2,.182E-2,.138E-2,.109E-2,.454E-3/
      DATA(ATTAB(I,4),I=1,27)/5.35,5.41,5.48,5.56,5.65,5.76,5.89,
     16.01,6.02,5.83,5.49,5.08,3.29,1.60,
     21.05,.239,.0750,.0280,.0132,.981E-2,.758E-2,
     3.605E-2,.495E-2,.351E-2,.262E-2,.204E-2,.829E-3/
      DATA(ATTAB(I,5),I=1,27)/9.35,9.44,9.56,9.70,9.86,10.05,10.30,
     110.58,10.80,10.69,10.53,9.81,7.13,3.94,
```

```
                22.70,.698,.245,.0920,.0399,.0282,.0209,
                3.0161,.0128,.867E-2,.631E-2,.482E-2,.186E-2/
                 DATA(ATTAB(I,6),I=1,27)/14.27,14.40,14.58,14.79,15.03,15.33,15.71,
                116.18,16.67,16.70,16.38,15.81,12.36,7.51,
                25.38,1.52,.591,.236,.100,.0686,.0488,
                3.0362,.0279,.0180,.0127,.947E-2,.348E-2/
                 DATA(ATTAB(I,7),I=1,27)/21.78,21.97,22.24,22.54,22.90,23.36,23.9 ,
                124.68,25.61,25.89,25.70,2 .14,20.39,13.87,
                210.37,3.23,1.38,.602,.265,.179,.124,
                3.0892,.0661,.0399,.0227,.0193,.661E-2/
                 DATA(ATTAB(I,8),I=1,27)/33.22,33.49,33.88,34.32,34. ,35.59,36.40,
                137.55,39.18,39.84,39.96,39.50,34.54,24.83,
                219.40,6.36,3.09,1.49,.706,.486,.338,
                3.239,.172,.0970,.0607,.0416,.0128/
                 DATA(ATTAB(I,9),I=1,27)/42.48,42.82,43.30,43.84,44.51,45.53,46.47,
                147.93,50.16,51.10,51.54,51.22,45.94,34.46,
                227.59,10.06,4.86,2.49,1.24,.872,.613,
                3.435,.313,.171,.103,.0677,.0190/
                 DATA FACTOR/1.0,1.0,1.0,1.0,1.0,0.99,0.99,1.0,1.01,1.02,
                11.02,1.01,1.0,1.0,1.0,1.09,1.02,1.0,1.0,0.99,
                21.55,1.25,1.0,0.81,0.65,1.72,1.29,1.0,0.79,0.64,
                31.0,1.0,1.0,1.0,1.0,1.0,1.0,1.0,1.0,1.01,
                41.01,1.01,1.0,0.99,0.98,0.95,0.96,1.0,1.05,1.10,
                51.28,1.14,1.0,0.85,0.72,1.73,1.30,1.0,0.79,0.64,
                61.0,1.0,1.0,1.0,1.0,1.0,1.0,1.0,1.0,1.01,
                71.02,1.01,1.0,0.99,0.97,0.96,0.97,1.0,1.04,1.07,
                81.04,1.03,1.0,0.95,0.88,1.74,1.30,1.0,0.79,0.63,
                91.0,1.0,1.0,1.0,1.0,1.0,1.0,1.0,1.0,1.01,
                11.02,1.01,1.0,0.98,0.97,0.99,0.99,1.0,1.02,1.04,
                20.91,0.96,1.0,1.01,1.01,1.75,1.31,1.0,0.78,0.62,
                31.0,1.0,1.0,1.0,1.0,1.0,1.0,1.0,1.0,1.01,
                41.03,1.01,1.0,0.98,0.97,1.01,1.0,1.0,1.0,1.01,
                50.88,0.95,1.0,1.04,1.06,1.72,1.31,1.0,0.78,0.62/
                 DATA RATLIM /.05/
           C         GIVE ZERO ATTN IF RATE FALLS BELOW LIMIT
                 IF(RATE.GT.RATLIM) GO TO 12
                 GMRAIN = 0.
                 RETURN
              12 WVLTH = 29.979/FREQ
                 JMAX=3
                 IF(WVLTH.GT.WVLTAB(1)) GO TO      14
                 ILOW=0
                 JMAX=2
                 GO TO 18
           CCC   THIS DO LOOP IS 2 LESS THAN NO. OF WVLTAB INPUT
              14 DO 15 I=2,25
                 IF(WVLTH.LT.(.5*(WVLTAB(I)+WVLTAB(I+1)))) GO TO 16
              15 CONTINUE
           CCC   SET ILOW EQUAL TO 1 LESS THAN DO MAX
                 ILOW=24
                 GO TO 18
              16 ILOW = I-2
              18 CONTINUE
                 DO 190 I=2,7
                 IF (RATE. LT.(.5*(RATTAB(I)+RATTAB(I+1))))GO TO 195
             190 CONTINUE
                 KMIN=6
```

```
                GO TO 198
            195 KMIN=I-2
            198 CONTINUE
                DO 20 J=1,JMAX
                IJ = ILOW + J
                X(J) = -ALOG(HVLTAB(IJ))
             20 CONTINUE
      C            INTERPOLATE
                Z = -ALOG(HVLTH)
                DO 25 K=1,3
                KJ=KMIN+K
                RATES(K)=RATTAB(KJ)
                DO 24 J=1,JMAX
                IJ = ILOW + J
                Y(J)=-ALOG(ATTAB(IJ,KJ))
             24 CONTINUE
                ATTN(K)=EXP(-AITK(X,Y,Z,JMAX) )
             25 CONTINUE
      C            APPLY TEMPERATURE CORRECTION
                DO 31 I=2,5
                IF(T.LT.TMPTAB(I)) GO TO 33
             31 CONTINUE
                ILOW = 4
                GO TO 35
             33 ILOW = I-1
             35 CONTINUE
                DO 41 J=2,6
                IF(HVLTH.LT.TLMDA(J)) GO TO 43
             41 CONTINUE
      CCC       JLOW IS 2 LESS THAN DO WAT
                JLOW=4
                GO TO 45
             43 JLOW = J-2
             45 CONTINUE
                DO 50 K=1,2
                DO 49 J=1,2
      C            INTERPOLATE IN TEMPERATURE
                KJ=(KMIN/2)+K
                JI = JLOW + J
                FAC = ((TMPTAB(ILOW)-T)*FACTOR(ILOW+1,JI,KJ)+(T-TMPTAB(ILOW+1))*
               1 FACTOR(ILOW,JI,KJ))/(TMPTAB(ILOW)-TMPTAB(ILOW+1))
                JI = JLOW +3-J
                FACIT(J) = (TLMDA(JI)-HVLTH)*FAC
             49 CONTINUE
                TFACT(K) = (FACIT(2)-FACIT(1))/(TLMDA(JLOW+1)-TLMDA(JLOW+2))
             50 CONTINUE
      C            COMPUTE ATTENUATION (DB/KM)
                KJ=2*(KMIN/2)+1
                GMRAIN=AITK(RATES,ATTN,RATE,3)*
               1((RATE-RATTAB(KJ))*TFACT(2)+(RATTAB(KJ+2)-RATE)*
               2TFACT(1))/(RATTAB(KJ+2)-RATTAB(KJ))
                RETURN
                END
```